PREPRINT TEXT. Morzaria-Luna, H.N., C.H. Ainsworth, J.H. Tarnecki, and A. Grüss. 2018. Diet composition uncertainty determines impacts on fisheries following an oil spill. Ecosystem Services. 33(Part B):187-198, 10.1016/j.ecoser.2018.05.002

Diet composition uncertainty determines impacts on fisheries following an oil spill

Hem Nalini Morzaria-Luna[1*]

Cameron H. Ainsworth[2]

Joseph H. Tarnecki[3]

Arnaud Grüss[4]

1) CEDO Intercultural, PO Box 44208, Tucson, AZ 8573, USA. Edif. Agustín Cortés, s/n. Puerto Peñasco, Sonora CP 83550, México.
2) College of Marine Science, University of South Florida, 140 7th Avenue South, St. Petersburg, FL 33701, USA. E-mail: ainsworth@usf.edu. Phone: (727) 553-3373
3) Florida Fish and Wildlife Conservation Commission, Fish and Wildlife Research Institute, 100 8th Ave SE, St. Petersburg, FL 33701, USA. E-mail: jtarnecki83@gmail.com. Phone: 941 875-1247
4) Department of Marine Biology and Ecology, Rosenstiel School of Marine and Atmospheric Science, University of Miami, 4600 Rickenbacker Causeway. Miami, FL 33149-1031, USA. E-mail: agruss@rsmas.miami.edu. Phone: (305) 421 4262

* Corresponding author. hmorzarialuna@gmail.com

Visiting researcher at the Northwest Fisheries Science Center, NOAA, 2725 Montlake Blvd. E., Seattle, WA 98112, USA

Abstract

Oil spills can disrupt marine and coastal ecosystem services leading to reduced employment opportunities and income. Ecosystem models can be used to estimate the effects of oil pollution; however, uncertainty in model predictions may influence damage assessment. We performed an uncertainty analysis for the Atlantis ecosystem model of the Gulf of Mexico (Atlantis-GOM), under a scenario simulating the effects of the *Deepwater Horizon* oil spill. Atlantis-GOM simulates major biophysical processes, including the effects of oil hydrocarbons on fish growth and mortality. We used all available fish stomach content data to inform parameter distribution for the Atlantis-GOM availability matrix, which represents predator total consumption potential and diet preference. We sampled the fish diet composition distribution and analyzed the variability of functional group biomass and catch predicted by Atlantis-GOM simulations to changes in the availability matrix. Resulting biomass and catch were then used to fit statistical emulators of the ecosystem model and predict biomass and catch given the complete diet parameter space. We used simulated and emulated data to assess changes in recovery time to oil spill effects. Uncertainty in diet composition had large effects on model outputs and may, therefore, influence damage assessment of oil exposure on economically important species.

Keywords

Oil hydrocarbons; Food web; Uncertainty analysis; Gulf of Mexico; Atlantis ecosystem model

1. Introduction

Human survival and well-being depend on marine and coastal ecosystem services (Costanza *et al.* 1997); and thus are also dependent on management and conservation of the ecosystems that provide these services (Liquete *et al.* 2013). Marine and coastal systems provide a variety of ecosystem services including provisioning (e.g. fisheries), regulation and maintenance (e.g. coastal storm and flood protection), support (eg. primary production), and cultural services (Millenium Ecosystem Assessment 2006, Liquete *et al.* 2013). Importantly, fisheries provide some of the most important and lucrative ecosystem services through the production of seafood. Human-related stressors threaten food provisioning; oil spills in particular can cause catastrophic damages because they are unpredictable in space and time and the people and equipment necessary to minimize their negative impacts might not be readily available (Silliman *et al.* 2012). Accidental oil spills have caused extensive economic impacts to fisheries through massive fish and invertebrate die-offs, fishery closures, or decreased consumer confidence in seafood quality or safety (Committee on the Effects of the Deepwater Horizon Mississippi Canyon-252 Oil Spill on Ecosystem Services in the Gulf of Mexico *et al.* 2014). As offshore, deep-water oil exploration expands, large oil spills are likely to occur in the future and lead to long-lasting and unexpected ecosystem-level effects (Pettingill & Weimer 2002).

Furthermore, the exposure of marine organisms to oil may lead to sublethal effects such as carcinogenicity, mutagenicity, cellular damage, endocrine disruption, and reduced survival (Larsen *et al.* 2016). These effects may all occur even at very low oil concentrations (Nahrgang *et al.* 2016). Oil-derived compounds may penetrate the marine food web when organisms ingest oil droplets or oil-coated food, or when oil contacts respiratory surfaces (Farrington *et al.* 2016). However, analyses of stable isotope ratios, which represent time-integrated information on consumers' diet, have found that oil assimilation in animal tissues was limited in areas affected by oil spills (Han *et al.* 2015). Nonetheless, oil exposure may lead to structural food web shifts, favoring species that can readily metabolize hydrocarbons (Passow & Hetland 2016), and hydrocarbons might slow the growth of marine animals, increase their mortality rates, and propagate toxicity effects across the food web (Perhar & Arhonditsis 2014). The indirect food web effects of oil exposure, determined by resource availability (Passow & Hetland 2016), may lead to disturbances at higher-trophic levels and to trophic cascades, where predators reduce prey abundance, which then releases the prey's food from control (Peterson *et al.* 2003).

End-to-end ecosystem models that can simulate direct mortality events, bioaccumulation of oil-related contaminants, and the indirect effects of oil pollution on ecosystem components via ecological interactions can be used to understand the long-term effects of oil pollution on ecosystem structure (De Laender *et al.* 2011). A variety of existing ecosystem modeling platforms combine physicochemical and oceanographic processes with trophic interactions and, therefore, have the ability to simulate the effects of natural and human-related stressors (see Plagányi 2007, O'Farrell *et al.* 2017 for a review). However, ecosystem models are fraught with uncertainty, including parameter uncertainty (Link *et al.* 2012); these models require hundreds to thousands of parameters which, in most cases, cannot be measured exactly or are unknown (Grüss *et al.* 2016). Consequently, any decisions or management actions taken based on ecosystem model predictions will be highly uncertain and be accompanied by associated tradeoffs. It is therefore important to understand and quantify the sources of uncertainty in ecosystem model predictions, including how uncertainty in model outputs relates to uncertainty in model inputs (Saltelli *et al.* 2008), such that the conclusions drawn from ecosystem model predictions are robust and transparent (Urrego-Blanco *et al.* 2016). Uncertainty analysis can be used to determine the variability (prediction imprecision) in the outcome variable that is due to the uncertainty in estimating the values of the input parameters (Iman & Helton 1988); while a

sensitivity analysis extends the uncertainty analysis by identifying which input parameters are important in altering the value of the outcome variable (Blower & Dowlatabadi 1994). End-to-end ecosystem models are generally highly complex and use large volumes of simulation data such that it is rarely feasible to conduct detailed uncertainty or sensitivity analyses for them (Allen & Fulton 2010; but see Köhler & Wirtz 2002, Niiranen *et al.* 2012, Lassalle *et al.* 2014, Morris *et al.* 2014, Mateus & Franz 2015). However, statistical emulation can be used to model the input-output relationships of an ecosystem model in a computationally-efficient manner; this technique creates a surrogate ecosystem model which acts as a fast approximation of the original model and can be employed to explore parameter uncertainty (Mattern *et al.* 2013).

In the present study, we apply an uncertainty analysis to examine how uncertainty in diet composition of an end-to-end ecosystem model affects determination of oil spill impacts on food provisioning ecosystem services in the Gulf of Mexico, a Large Marine Ecosystem bordered by the U.S., Mexico and Cuba, using fisheries catch and recovery time of target fish biomass as indicators. We employed the Gulf of Mexico Atlantis ecosystem model (Atlantis-GOM), which is an application of the Atlantis modeling platform. Atlantis is a sophisticated, three-dimensional deterministic modeling platform which simulates oceanography, ecology, fisheries dynamics, human impacts, and resource management (Fulton, Parslow, *et al.* 2004, Fulton *et al.* 2011). Atlantis outputs can be used to derive ecosystem indicators, quantitative measures that can be used to analyse the response of ecosystem services to simulated perturbations in a similar way as indicators in a real system (Smith *et al.* 2015, Reed *et al.* 2017). Because Atlantis is a deterministic model, output is completely determined by the input parameters and structure of the model; the only uncertainty affecting the output is generated by input variation (Marino *et al.* 2008). The Atlantis-GOM model was primarily designed to assess the food web impacts of the *Deepwater Horizon* oil spill (Ainsworth *et al.* 2015), which, in 2010, released an estimated 4.9 million barrels of crude oil (±10%) from the base of the continental shelf in the Northern Gulf of Mexico (Murawski *et al.* 2016). Atlantis-GOM represents the state of the Gulf of Mexico in 2010 ('baseline conditions'), and can simulate the direct effects of oil spills and their indirect effects via trophic interactions to ultimately determine the impact on ecological communities and ecosystem services decades after the spill (Coleman *et al.* 2014).

2. Methods

We evaluated the uncertainty in assessing the impacts of oil hydrocarbons predicted by Atlantis-GOM to the assumed food web structure. We incorporated new fish stomach content data to the Atlantis-GOM diet matrix, notably data originating from the northern and western Gulf of Mexico (Simons *et al.* 2013). We used this data to obtain robust diet composition estimates and associated errors for the Atlantis-GOM by bootstrapping aggregate fish diets from stomach sampling and online sources, and feeding the resulting data into a statistical model. We then employed the distribution of diet compositions and associated errors predicted by the statistical model to bound uncertainty in the Atlantis-GOM availability matrix. Previously, Ainsworth et al. (2018) explored the impacts of direct oil exposure on fish growth and mortality, the impacts of ichthyoplankton contamination on recruitment success, and the impacts of fishery closures on the GOM food web. We apply their worst-case scenario of direct oil exposure on fish growth and mortality to estimate how the effects of the oil spill on exploited species biomass, ecosystem indicators, and fisheries is influenced by diet composition uncertainty. We then employed statistical emulators that are less computationally demanding than the Atlantis model itself to examine the complete distribution of availability parameter estimates. Finally, we examine fish catch and recovery time of target fish biomass using simulated and emulated outputs.

Each of the abovementioned stages is described in detail below. All analyses were carried out in the R statistical framework (R Core Team 2017); the packages used are described in Table S1. We employed virtual machines running on the Microsoft Azure cloud computing platform (Standard F16 series, 16 cores, 32 GB memory) using Ubuntu 16.04; we ran parallel simulations using a total of 15 machines (for a total of 240 cores). The specifications to customize the virtual machines for Atlantis-GOM simulations and the R code used to generate the simulations and the statistical emulators, analyze data, and generate figures is freely available in GitHub https://github.com/hmorzaria/atlantis_gom_oil. The biomass and fish catch outputs from the Atlantis-GOM model simulations can be utilized to replicate our figures and are available from the Gulf of Mexico Research Initiative Information & Data Cooperative (GRIIDC) repository at https://data.gulfresearchinitiative.org/data/R6.x805.000:0002 [DOI:10.7266/N71G0JSG]

2.1. The Atlantis modeling platform and the Atlantis-GOM model

Atlantis is an end-to-end ecosystem modeling approach that represents all trophic levels from bacteria to apex predators and humans. Atlantis process equations can be found in Fulton (2001), Fulton, Parslow, *et al.* (2004), and Fulton, Smith, *et al.* (2004); further information can be found in the Atlantis User's Guide (Audzijonyte *et al.* 2017), recently published papers reporting Atlantis applications (Smith *et al.* 2015, Nyamweya *et al.* 2016), as well as in the Atlantis Wiki (https://research.csiro.au/atlantis/home/links/). Atlantis integrates physical, chemical, ecological, and fisheries dynamics in a three-dimensional, spatially-explicit domain that uses an irregular polygon structure to represent important bioregional features while saving computation time in homogeneous space. The modeling platform summarizes biological components as functional groups aggregated by trophic, life history, or niche similarities. Atlantis polygons aim to capture important climatic, biophysical, or jurisdictional features. In Atlantis, numerous sub-models simulate features and processes crucial to ecosystem structure and functioning, including biochemistry (e.g., nutrient cycling, salinity, oxygen availability), food-web interactions, fisheries, dependence of functional groups on biogenic and physical habitat, and physical and biophysical features (e.g., light penetration, temperature, stratification). Atlantis therefore bridges low and high trophic level drivers and processes. The versatility of this modeling platform allows simulating important physical processes and their impacts on fish and fisheries in a way inaccessible to simpler modeling frameworks. This comprehensive modelling approach is particularly useful in marine ecosystems like the GOM, where exogenous nutrient and freshwater inputs and oceanographic processes have a major structuring influence on species distributions and productivity.

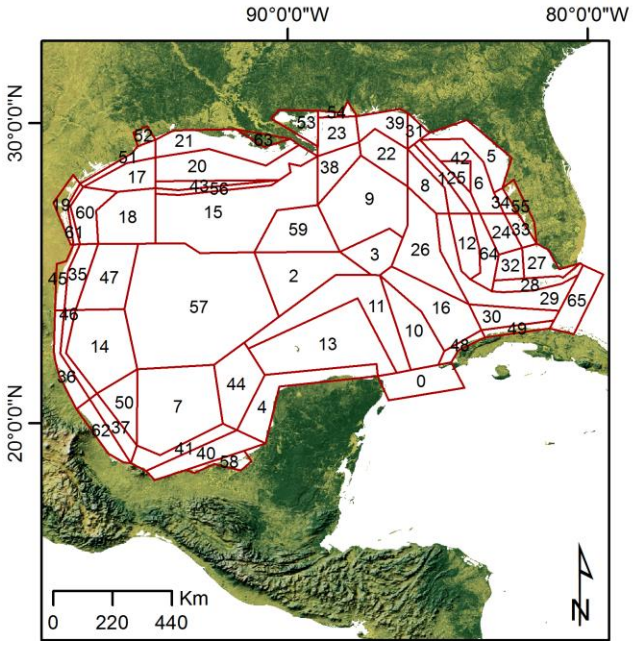

Figure 1. Extent and polygon configuration of the Atlantis ecosystem model for the Gulf of Mexico (Atlantis-GOM).

The Atlantis-GOM model was designed to understand the food web impacts of the *Deepwater Horizon* oil spill, and to evaluate the effectiveness of marine protected area networks, the toxicological effects of red tide (*Karenia brevis*; a type of harmful algal bloom) and the performance of harvest control rules (Drexler & Ainsworth 2013, Masi *et al.* 2014, Ainsworth *et al.* 2015). The model features, parameters, and driving data are described in detail in Ainsworth et al. (2015). Briefly, Atlantis-GOM polygon geometry (Figure 1) follows circulation, habitat features, and management divisions in the Gulf of Mexico. In each Atlantis-GOM polygon, there are up to six water column layers and one sediment layer. Atlantis-GOM simulates food web dynamics using 91 functional groups; important species (e.g., managed species, species of conservation interest, or functionally important species) tend to be assigned a dedicated functional group, while other species are treated in aggregate. Functional groups of the Atlantis-GOM model include: reef fish (11 groups), demersal fish (12), pelagic fish (15), forage fish (4), elasmobranchs (6), shrimps (4), seabirds (2), mammals (4), sea turtles (3), commercial benthos (3), structural species (4), macrobenthos (3), filter feeders (3), primary producers (8), pelagic invertebrates (4), and nutrient cyclers (4, including two detritus groups). The biomass of each of these functional groups is allocated over the spatial domain of Atlantis-GOM following predictions of abundance based on environmental conditions (Drexler & Ainsworth 2013). Nutrient flux and passive oceanic transport in Atlantis-GOM are driven by the American Seas model (AMSEAS) based on the National Research Laboratory-developed Navy Coastal Ocean Model (NCOM) (Martin 2000). The Atlantis-GOM model is initialized for 2010 and the simulations operate at 12-hour time steps.

The Atlantis modeling platform relies on 'availability' parameters rather than diet proportions; these parameters are scaling values in a Holling Type II predator-prey functional

response. Availability reflects predator total consumption potential and diet preference; it is sensitive to functional group aggregation, predator and prey abundances, and spatial co-occurrence among other factors. The availability matrix represents both adult and juvenile predator ontogenetic stages consuming both juvenile and adult prey. Masi et al. (2014) constructed the initial diet matrix of Atlantis-GOM using probabilistic analysis of gut contents. Later, Tarnecki et al. (2016) revised the Atlantis-GOM diet matrix using the same approach but a larger amount of diet data. Tarnecki et al. (2016)'s findings were used to modify the patterns of connectivity in the Atlantis-GOM model, in particular to add new trophic linkages while maintaining the absolute flows derived from the tuning process carried out in Ainsworth et al. (2015), as the behavior of the Atlantis-GOM model was still realistic. Thus, (Ainsworth *et al.* 2018) employed a diet matrix over-represented by eastern GOM diet data (e.g., extensive collections were provided by the Florida Wildlife Commission, (Masi *et al.* 2014, Ainsworth *et al.* 2015) when simulating the impacts of the *Deepwater Horizon* oil spill.

2.2 Diet composition

Here, we updated the fish diet composition in the Atlantis-GOM model from Tarnecki et al. (2016), to incorporate newly-available data from the northern and western GOM and thus identify previously missing predator-prey linkages. We combined data on feeding ecology from the literature and empirical studies. We analyzed a total of 21,153 samples of adult fish, a nearly 20% increase over Tarnecki et al. (2016)'s 17,719 samples. The sources of the diet data are provided in Table S2. A food web diagram illustrating the updated predator–prey connectivity in the Atlantis-GOM ecosystem model is shown in Figure 2, and is based on hierarchical clusters of diet composition (Figure S1).

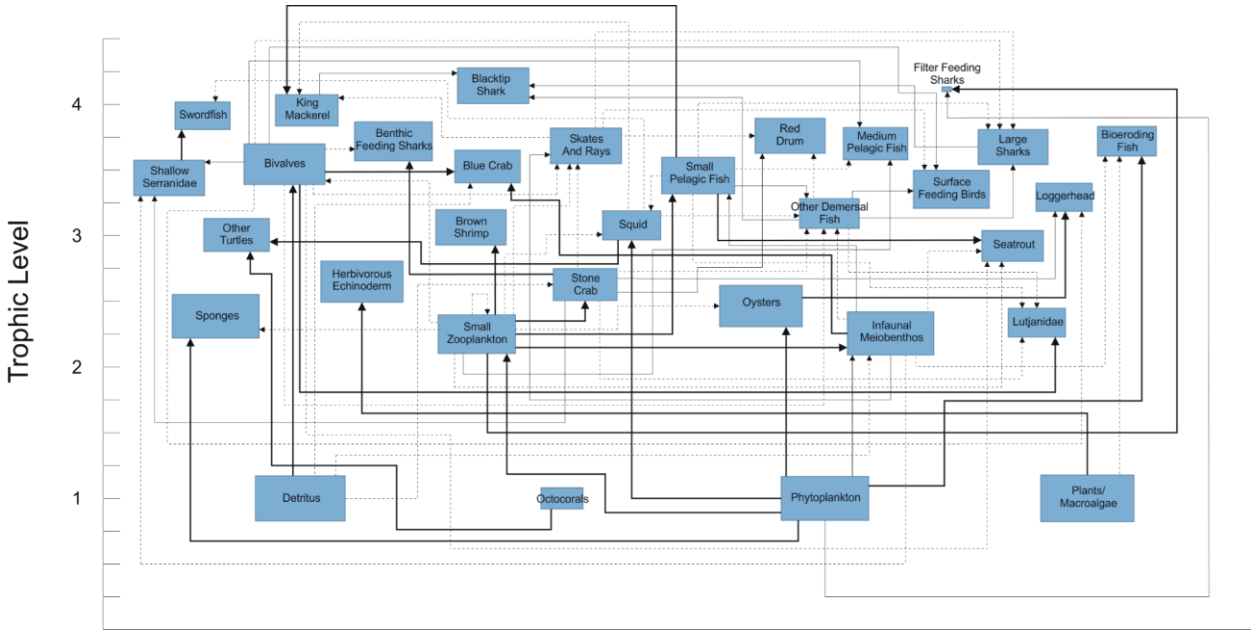

Figure 2. Food web diagram illustrating predator–prey connectivity in the Atlantis-GOM ecosystem model. Each box represents a cluster from a hierarchical cluster analysis (Figure S1) on the diet data and is named after the predator functional group containing the highest biomass estimates (coming from (Drexler & Ainsworth 2013). Box sizes are proportional to area log

biomass estimates. Arrows indicate the flow of energy from prey to predators. Dotted lines indicate functional groups with ≥10% − 20% prey contributions, thin solid lines represent prey contributions ranging from >20% − 40%, and thick solid lines indicate >40% prey contributions. Diets <10% were omitted from the food web diagram. The Y-axis indicates the estimated trophic level of each grouping.

Secondly, we fed the diet data we had gathered into a statistical model based on the Dirichlet distribution in order to quantify the likely contributions of prey to predators' diet (Ainsworth *et al.* 2010, Tarnecki *et al.* 2016). The Dirichlet function is the multivariate generalization of the beta function; the marginal beta distributions provide a mode representing the most frequently observed diet proportion for a given predator–prey combination in percentage wet weight, as well as confidence intervals that reflect diet variability and data quality and better account for the uncertainty surrounding rare feeding events. It is important to consider rare predator-prey interactions, because even a very small contribution of a prey item to a predator's diet can be important when the biomass and consumption rates of the predator are very large and/or the biomass of the prey item is very small (Walters et al. 2008). Also, weak diet linkages can become more important in a predator's diet over time if prey availability changes. The predator diets were normalized and organized in a matrix where columns represented all Atlantis-GOM functional groups except the two detritus groups and rows were individual stomach samples or integrated diet composition (i.e. predator averages taken from FishBase). We eliminated empty stomachs to create a time-integrated diet composition with fewer zero-value prey items. We bootstraped 10,000 of these samples with replacement and fit the bootstrapped values to the Dirichlet density function using a maximum likelihood fitting procedure (Ainsworth *et al.* 2010, Masi *et al.* 2014, Tarnecki *et al.* 2016).

2.3 Oil spill scenario

Ainsworth et al. (2018) simulated impacts from the *Deepwater Horizon* oil spill and subsequent ecosystem recovery over a 50-year time horizon. The methodology used by Ainsworth et al. (2018) applies dose-response relationships to predict growth rate impacts and mortality rate impacts. Two parameters set the magnitude of oil effects. The first is a concentration factor (K) that relates water column concentration data (i.e., from hydrodynamic oil transport modeling) to dose-response relationships conditioned on sediment concentrations. The second is a polycyclic aromatic hydrocarbon (PAH) concentration threshold (β) below which the 'hockey-stick' style dose-response relationship for mortality predicts no adverse effect. The growth relationship uses a low threshold and so a growth effect is always present to some degree in oiled areas. In the present study, we used values for K and β corresponding to the most severe oil impact scenario tested by Ainsworth et al. (2018)[K1000 β363] scenario. This scenario assumes a 1000x concentration factor between water column and sediment oil and a dose response threshold for mortality effects of 363 ppb PAH. This severe effect scenario was selected for the present study to make ecosystem impacts obvious and to support the heuristic interpretation of qualitative results. However, note that this high level of effect is not unrealistic. Under this scenario, Ainsworth et al. (2018) successfully recreated observed population declines in reef systems. We employed a 100-day "spin up" period before introducing oil in Atlantis-GOM to allow for transient dynamics to stabilize in the model. Oil forcing lasted for 167 days, followed by a 20-day depuration period that represents 99% clearance via gill elimination, metabolic transformation, fecal egestion, growth dilution and elimination via egg deposition and sperm ejection.

2.4 Uncertainty analysis

The Atlantis-GOM availability matrix includes over 2500 input parameters that define the relative contribution of each of the functional groups represented in model to each predator diet. In practice, exploring the full parameter space is computationally prohibitive because of Atlantis' long run time (approximately 48 hours for a 30 year simulation for Atlantis-GOM). Therefore, initially, we sampled the fish diet composition estimates (described in Subsection **2.2**) and used these randomized subsets to create 1000 availability matrices that were used in the uncertainty analysis. We sampled the diet composition estimates using a Latin hypercube design, which is a generalization of a Latin square to an arbitrary number of dimensions (Shields & Zhang 2016). This approach subdivides the sample space in equal areas *a priori* and then samples randomly within each subdivision ensuring that the random samples represent the parameter space (Prowse *et al.* 2016). To convert diet composition estimates (i.e., the proportions of each predator's diet consisting of each prey functional group) to the matrix of availability parameters required by the Atlantis functional response, we used two methods: (1) When the diet data represented a predator-prey interaction not previously described in the Atlantis diet matrix, the diet composition value was divided by 1000 and included in the availability matrix. This convention, used in previous Atlantis applications (Brand *et al.* 2007, Ainsworth *et al.* 2011), puts the value within the correct order of magnitude relative to other linkages and provides a suitable starting point for tuning. (2) When the diet data represented a predator-prey interaction that already existed in the availability matrix, the existing diet availability parameter was increased or decreased by an amount proportional to the difference between random draw and the mode of the marginal beta distribution. For example, if the random draw resulted in a doubling of the diet value relative to the most likely diet value (Table S3), then the availability in the model was also doubled. Since the diet samples considered in this study include only adult stages, we randomized only the diets of adult predators and modified the proportions of juvenile and adult prey equally to retain the ratio between them. The randomized availability matrices that varied the diet composition of all predators simultaneously were then employed in a 1,000-member computer experiment ensemble. We ran 1,000 Atlantis-GOM simulations over a 15-year time horizon (2010-2025), in 12-hour time steps.

Secondly, we built statistically-based representations of Atlantis, known as "emulators" or "metamodels", that approximate the complex function linking the model outputs Y to its inputs X, $Y = f(X)$, using a simpler mathematical function $\eta(X) \approx f(X)$ from a set of training data points (Guillaume & Guillaume 2014). In our case the model outputs are functional group catch and biomass derived from the 1,000 ensemble of Atlantis-GOM simulations, both of these outputs directly relate to the effects of oil hydrocarbons on the food web; and the inputs are the availability values for randomized functional groups, each predator-prey interaction is a separate input. The emulator acts as a fast-running surrogate of the original model (Atlantis) that can be used to estimate model output for any set of inputs (Mattern *et al.* 2013). The emulator can be used to produce summary metrics that describe variance in the outputs due to variation in input parameters (Prowse *et al.* 2016). Since model structure and data determine which statistical technique is best, it is recommended to employ several statistical modeling approaches and to assess whether the patterns found generally agree between different statistical modeling techniques (Storlie *et al.* 2009). We compared six methods to derive the emulators: two regression methods (Generalized Linear Model, GLM, and bagged Multivariate Adaptive Regression Splines, BMARS); and four machine learning methods, including three tree-based models (Bagged Classification and Regression Trees, BCART, Random Forest, RF, and Boosted Regression Trees, BRT), and a neural network approach (the Extreme Learning Machine Learning, ELM). Regression models are useful to understand input-output relationships, but can suffer from lack of accuracy when model complexity increases (i.e. in

presence of nonlinearity or heterogeneity) (De Graaff *et al.* 2001). Machine learning gives better results than regression-based approaches when input-output relationships are complex, but creates black boxes that are difficult to interpret. Text S1 briefly describes each of the six methods applied to derive the emulators and the tuning parameters used for each. We developed emulators for each time-slice (i.e. each of the years of the 15-year simulation period). We divided the Atlantis-GOM simulations into training (75% of simulations) and testing (25%) data sets. We trained the model emulators on the training data and then scored model performance by applying the trained models to the test data, and examining the accuracy in predicting model outputs given the inputs. All emulators were optimized using 10 rounds of a 10-fold cross-validation, which determines the optimum fit for each fold and then estimates final model performance as the mean from the number of repeats (Kohavi 1995). We evaluated emulator performance using Taylor diagrams (Taylor 2001), which compare the accuracy of the different emulators using three related parameters in a single figure: standard deviation, correlation with observed data, and centred root mean square (RMS).

Third, we employed the full set of the cumulative marginal beta distribution describing diet matrix uncertainty to create 10,000 availability matrices using the general rules outlined above. We then used the statistical emulator with the best fit for each functional group and time slice to predict fish biomass and catch.

2.5 Analysis of Atlantis-GOM outputs

To understand how diet composition uncertainty influences the trophic effects of oil pollution predicted by the Atlantis-GOM, we compared simulated and emulated fish biomass and catch outputs to simulated outputs from the base model with no oil effects and the oil spill model from Ainsworth et al. (2018) which both use the base availability matrix from Tarnecki et al. (2016). We analyzed the following: (1) the simulated fish biomass and catch trajectories estimated from 1,000 Atlantis-GOM simulations; (2) emulator performance; (3) the emulated fish biomass and catch trajectories estimated from 10,000 emulations; (4) time to recovery, considered here as the time necessary to recover 99% of the initial biomass following the lowest biomass level ('*biomass minima*'), for both the simulated and emulated outputs. This stringent criteria was suitable for the Atlantis-GOM model results because of the monotonic biomass increases and mostly quick recovery times; and 5) performance of fisheries catch.

For ease of presentation, we show results for Atlantis-GOM fish functional groups aggregated into eight "guilds": elasmobranchs, groupers, large demersal fish, snappers, large pelagic fish, large reef fish, Sciaenidae, small demersal and reef fish, small pelagic fish, and snappers. The Atlantis-GOM functional groups that make up these guilds are presented in Table S4; a complete list of Atlantis functional groups and species in each group are provided in Ainsworth et al. (2015).

3. Results

3.1 Diet composition

The consideration of new fish stomach content data allowed us to identify a total of 126 new predator-prey interactions for the Atlantis-GOM ecosystem model. We identified new prey for 33 of the 47 fish functional groups represented in Atlantis-GOM; the number of new prey identified for each of these 33 groups varied between 1 and 10. The 126 new predator-prey interactions identified are illustrated in Figure S2. The most likely estimates (MLE) of prey contributions to predators' diet, their 95% confidence intervals, as well as the numbers of prey by fish functional groups are provided in Table S3. Figure S3 shows the percent diet

composition of Atlantis-GOM fish functional groups based on the diet analysis conducted in this study and Figure S4 describes differences in fish diet composition between Tarnecki et al. (2016) and the present study.

3.2 Uncertainty analysis

The simulated fish biomass (Figure 4), and catch (Figure 5) trajectories resulting from the 1,000 Atlantis-GOM simulations show that both biomass and catch outputs from the Atlantis-GOM model are highly sensitive to changes in availability parameter values, which define the relative contribution of each fish prey group to each predator diet. For example, for the large reef fish guilds (i.e., snappers, groupers, and Sciaenidae) as well as for the elasmobranch and small pelagic fish guilds, the magnitude of the impact of the oil spill scenario on biomasses varied up to 4-fold. An examination of the results for individual functional groups (Figures S5 and S6) reveal that these patterns are due to a few functional groups, including Seatrout, Small pelagics, Small demersal fish, and Pinfish.

Emulator performance, based on predicted values for each test data set by the six model emulators, was analyzed using Taylor diagrams, which quantify how closely each emulated biomass and catch patterns match simulated output (Figure 6). Emulated outputs that agree well with observations lie near the point marked "observed" on the X-axis in Figure 6. Models closest to this point, with the highest correlation and lowest RMS errors are considered to have the best performance. Figure 6 suggests a good predictive ability for biomasses for most of the model emulators; the model with the lowest performance was the Extreme Learning Machine. For the simulated catch, Random Forests, and, in some cases, Extreme Learning Machine models deviate from observations for most functional groups. Additionally, for certain functional groups, including Greater amberjack, Gag, Red drum and Seatrout, model correlations for catch are weaker than they are for biomass for most model emulators (Figure S7).

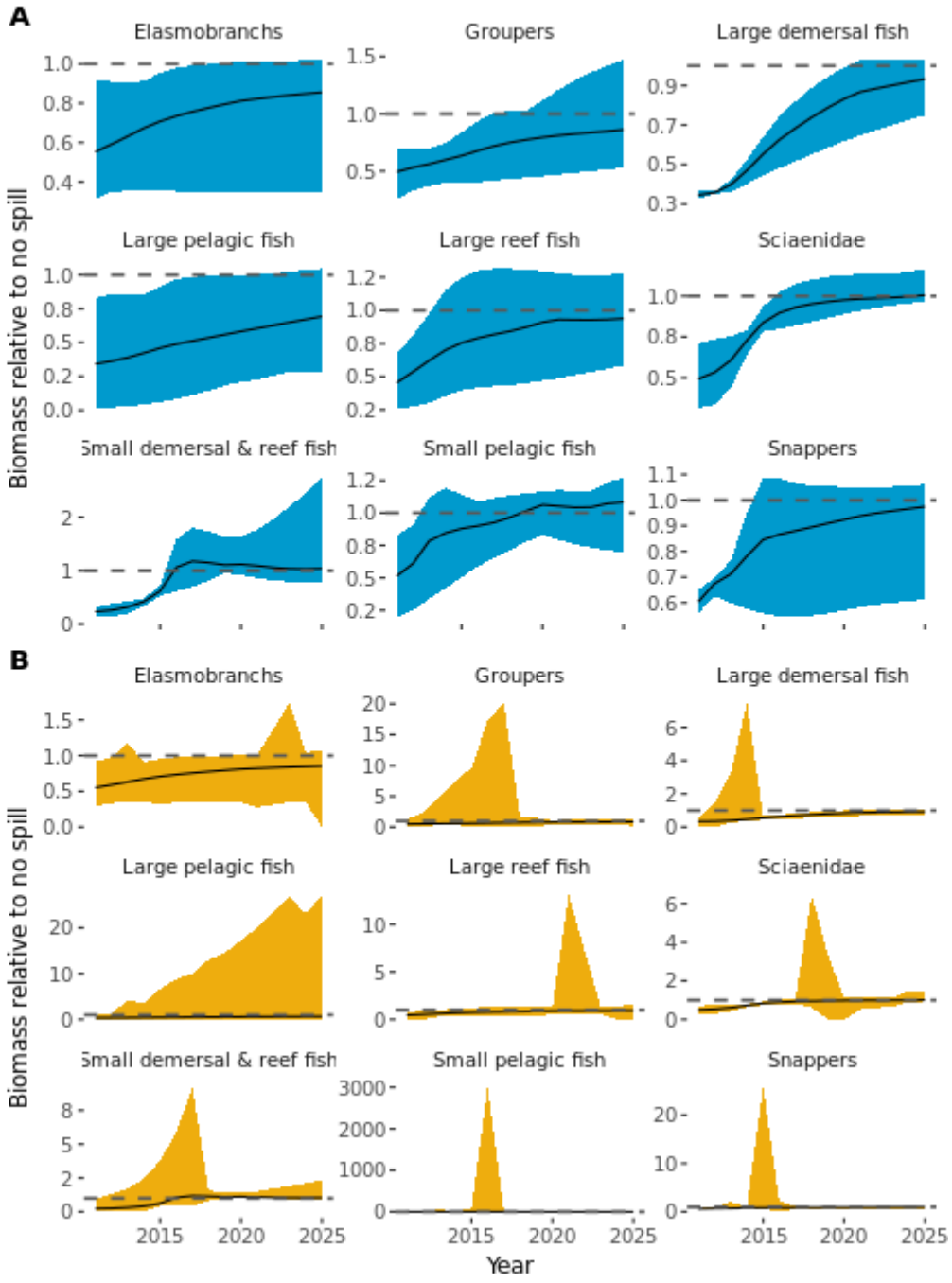

Figure 4. Simulated and emulated biomass trajectories for fish guilds. The shaded areas show the ranges of outcomes observed in the uncertainty analysis of the availability parameters, which were conducted using 1000 Atlantis-GOM ecosystem model simulations and 10,000 emulations. Note that for the same functional group, the scale of the Y-axis varies. Simulations were based on a sample of randomized availability matrices produced in this study and emulations used the complete beta distribution. The solid lines represent biomass trajectories for the base Atlantis-GOM model, which employs the availability matrix produced in Tarnecki et al. (2016).

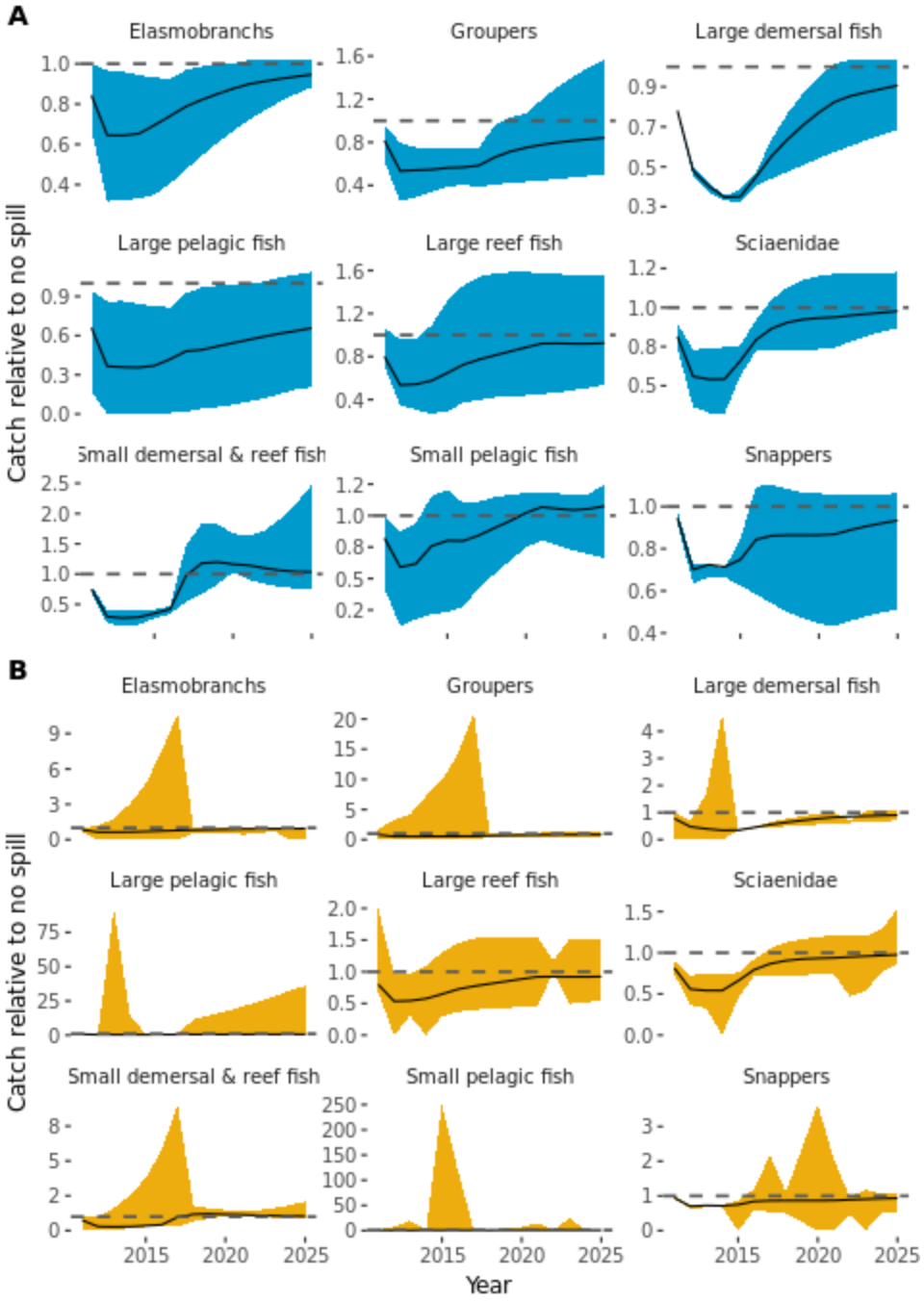

Figure 5. Simulated and emulated catch trajectories for fish guilds. The shaded areas show the ranges of outcomes observed in the uncertainty analysis of the availability parameters, which were conducted using 1000 Atlantis-GOM ecosystem model simulations and 10,000 emulations. Note that for the same functional group, the scale of the Y-axis varies. Simulations were based on a sample of randomized availability matrices produced in this study and emulations used the complete beta distribution. The solid lines represent biomass trajectories for the base Atlantis-GOM model, which employs the availability matrix produced in Tarnecki et al. (2016).

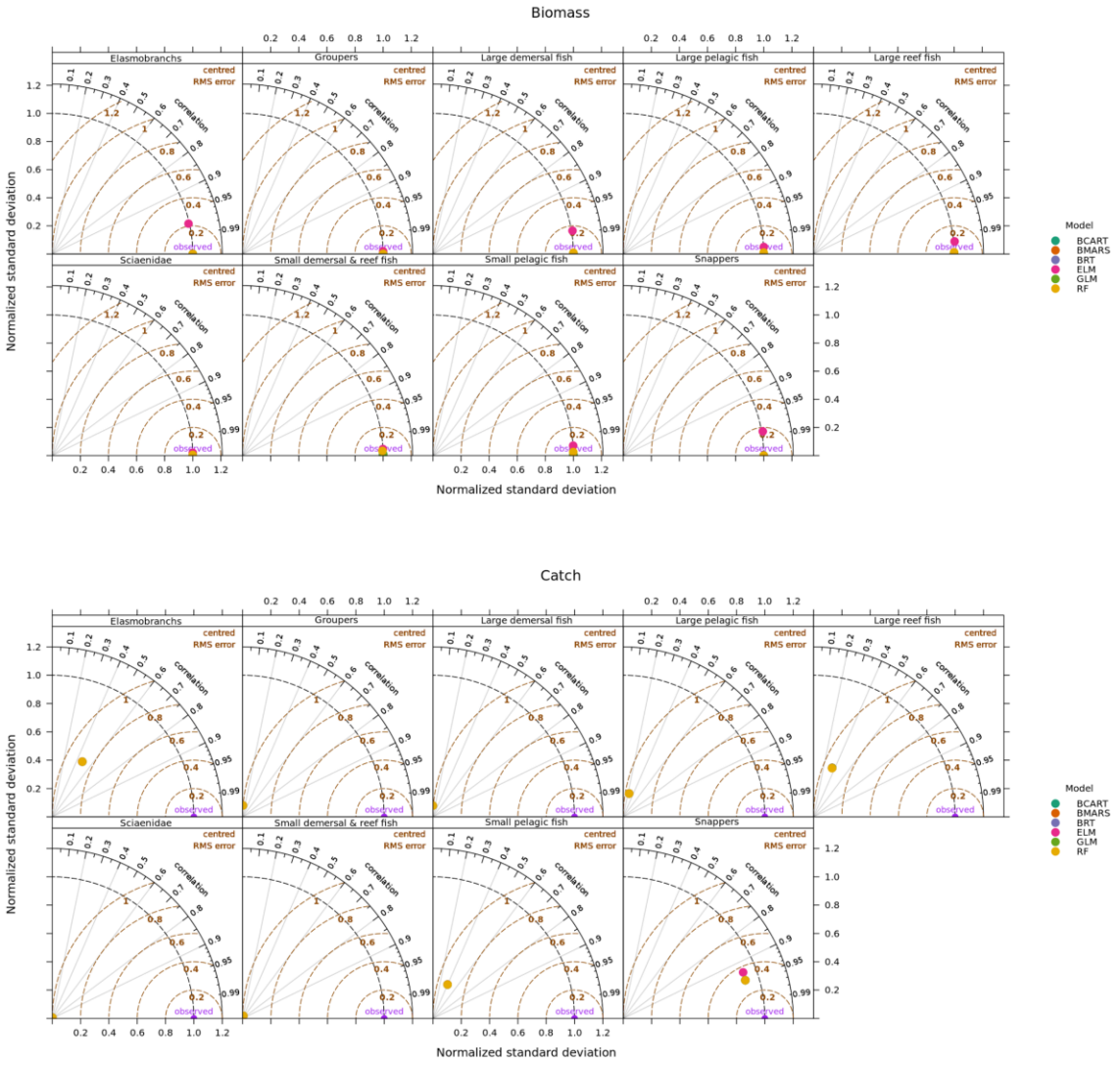

Figure 6. Taylor diagram examining emulator performance based on fish guild biomass and catch. The distance from the origin is the normalized standard deviation of Atlantis-GOM modeled biomass. The azimuth angle represents the correlations between the observed Atlantis-GOM simulations, and the distance between the each model symbol and the observations (1 at the X-axis) is the centred root mean square (RMS). The statistical models considered were: Generalized Linear Model (GLM), bagged Multivariate Adaptive Regression Splines (BMARS), bagged Classification and Regression Trees (BCART), Random Forest (RF), Boosted Regression Trees (BRT), and Extreme Learning Machine (ELM). Please refer to the online version of the article for color legend. The model markers that are not observed are stacked under the BRT marker on the X-axis.

The emulated fish biomass (Figure 4) and catch (Figure 5) trajectories resulting from the uncertainty analysis show that the Atlantis-GOM model is highly sensitive to changes in availability parameter values. Some guilds exhibited large ranges in biomass relative to the no oil spill scenario, with higher uncertainty in longer time horizons (e.g. Large pelagic fish). An examination of results for individual functional groups (Figures S5 and S6) reveal that for many functional groups, emulated biomass trajectory closely follows the biomass trajectory of the base Atlantis-GOM model (which uses the availability matrix from Tarnecki et al. 2016). Functional groups such as bioeroding fish, skates and rays, and large reef fish were resilient to changes in diet composition, although their diet is made up of multiple prey items (Table S4) and feeding linkages (Figure 2). It is likely that, in some instances, the randomized availability matrices values could have destabilized Atlantis-GOM before the simulation end time, or some functional groups could have gone extinct, while the emulators produces outputs regardless of the ecological implications. The range in emulated biomass and catch was not related to the number of diet samples used to inform the diet composition distribution (Figure S8).

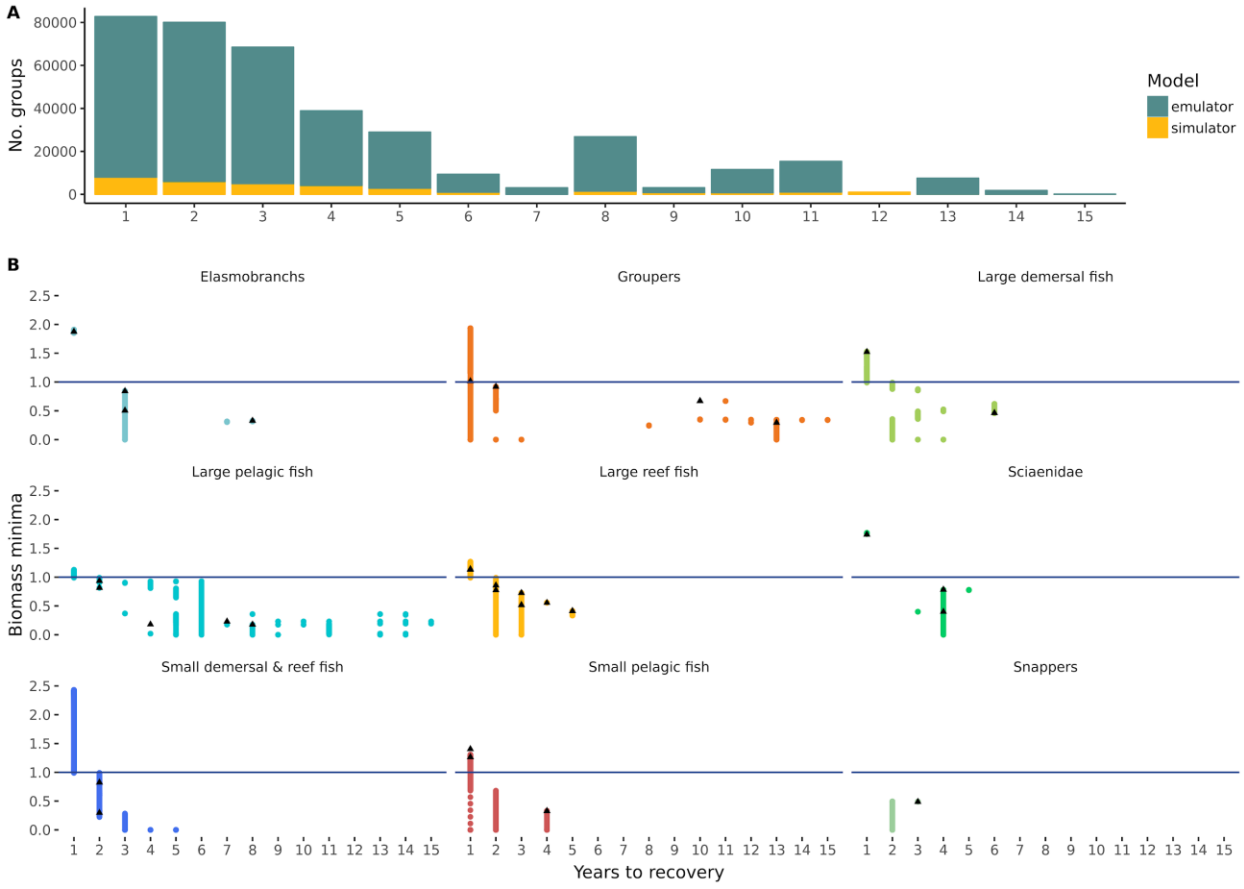

Figure 7. Target fish guild biomass recovery time from oil spill effects. A. Number of groups in simulated and emulated output that met the recovery criteria by year; recovery is defined here as a return to 99% pre-oil spill biomass. B. Biomass minima versus years to recovery. Points are simulated and emulated results and solid black triangles are base model.

3.3 Assessment of impacts of oil exposure

Recovery time, defined here as a return to 99% pre-oil spill biomass, varied widely within guilds, considering both the emulated and simulated data. In many cases, guilds did not recover within the 15-year time horizon, including most Large pelagic fish; guilds that did not recover were largely consistent across simulated and emulated data and the overall pattern of years to recovery by guild (Figure 7) followed the base model. However, there were fish groups that did not achieve recovery in the base model, but did under the simulated or emulated outputs (Table S5). Aggregated simulated catch per fleet (Figure S9), shows a smaller range of variation in response to oil spill compared to non-aggregated simulated catch, suggesting that both diet composition and the type of indicator used influence the assessment of oil spill impacts. Generally, model results exhibited a 20–30% reduction in catch relative to the no oil spill scenario. The largest losses were predicted in mackerel fisheries, reef handline and sport estuarine fisheries.

4. Discussion

As offshore, deep-water oil exploration expands worldwide, oil spills as large as the *Deepwater Horizon* spill are likely to occur in the future. Catastrophic oil spills have already impacted ecosystem services in marine systems (Garza-Gil *et al.* 2006, Soto *et al.* 2014). The *Deepwater Horizon* oil spill had large consequences for provisioning services, which contribute significantly to human well-being (Vilardy *et al.* 2011), including a significant profit loss that came from fishery closures and impacts on seafood demand (Murawski *et al.* 2014). Our simulation of oil spill effects using the Atlantis-GOM model found similar impacts on provisioning services, a decrease in biomass and catch of commercial target fish groups. Large pelagic species, groupers, and sciaenids suffered the highest decreases in biomass and catch as a result of oil effects. The uncertainty analysis implemented using 1,000 Atlantis-GOM simulations showed that predicted fish biomass and catch decreases in 2011 varied between -10% and over 60%. Thus, depending on the configuration of the availability matrix used, changes in fish biomass and catch were deemed strongly to mildly negative, or even slightly positive; although the variability in catch was dampened when using aggregated indicators such as catch per fleet. Resource managers are required to act on the best current knowledge in the face of uncertainty. Given this, the range of outcomes produced by the uncertainty analysis provides a general assessment of the reliability and precision of the model (Mattern *et al.* 2013) and can give provide decision-makers with information regarding possible outcomes, such that they can make well-justified choices (Uusitalo *et al.* 2015). Here we focused on catch as an indicator of provisioning services, however Atlantis model outputs can be used to estimate a variety of indicators of ecosystem services (Hayes *et al.* 2015, Smith *et al.* 2015); these indicators have focused on the effects of fishing because it is a major impact on marine ecosystems (Costello *et al.* 2010).

Atlantis models have been used to support Ecosystem Based Management worldwide (Fulton *et al.* 2011) and can be critical in assessing impacts such as oil spills (Ainsworth *et al.* 2018). However, the complexity and slow run times of applications of the Atlantis modeling platform have precluded formal uncertainty and sensitivity analyses. Previous studies using Atlantis ecosystem models have applied a scenario-based approach to account for uncertainty in model components (Kaplan *et al.* 2012, Perryman 2017) or have explored model sensitivity to a small number of parameters; for example, during development and validation of the Guam Atlantis Ecosystem Model, Weijerman (2015) performed sensitivity assessments of three parameters influencing primary productivity and coral growth by using the minimum and maximum parameter estimates to get boundaries for plausible trajectories. These approaches

explore a limited parameter space and may miss unintuitive and non-linear effects. The model simulations performed here help address this shortfall by examining a larger section of the parameter space. We took advantage of the flexibility in the Atlantis model structure, which allows exploration of structural uncertainty (Fulton *et al.* 2011), in combination with a cloud computing platform and parallel computing tools, to explore how assessment of oil spill recovery would change under multiple configurations of the Atlantis availability matrix, which describes food web relationships. Through this methodology, we ran 1000 Atlantis-GOM simulations in a reasonable amount of time (4 weeks); to our knowledge, this is the largest number of simulations ever carried out with any Atlantis model to explore a specific question. It remains computationally unfeasible to carry out a complete probabilistic analysis of Atlantis (i.e. eliciting prior distributions for parameters and updating them with the training set), but our targeted approach can explore a limited set of parameters of interest. These parameters can influence the behavior of multiple indicators of ecosystem services that can be derived from Atlantis model outputs such as biomass-weighted average weight of fish, an indicator of ecosystem structure and functioning; biomass-weighted average age of fish, which is a measure of system stability and resilience to perturbations; and proportion of predatory fish which reflects biodiversity and system resilience (Hayes *et al.* 2015, Smith *et al.* 2015).

We also developed emulators, low-order statistical approximations of the Atlantis-GOM model based on a limited number of Atlantis-GOM replicates. The emulators were used to predict the output of the Atlantis-GOM model at untried input settings. Emulator-based approaches are a computationally-efficient method for propagating uncertainty in model inputs to their outputs, since they enable exploration of how outputs depend on multiple possible parameter values (Mattern *et al.* 2013); this approach can render large experiments possible while eliminating the bias from testing a subset of the parameter space (Mattern *et al.* 2014). This is the first attempt to emulate a model built in the Atlantis Ecosystem Model framework, and can serve as a guideline on how to explicitly account for uncertainty in input parameters. Few studies have investigated uncertainty in coupled biological-physical ocean models (Cossarini *et al.* 2009, Béal *et al.* 2010, Mattern *et al.* 2013, 2014). The emulator results allowed us to examine which fish guilds and functional groups were more resilient to variability in the availability matrix. Quantifying the confidence that can be placed on model outputs and identifying influential parameters has important management implications (Morris *et al.* 2014). The emulator results showed that the effects of the inputs on the simulated outputs are highly non-linear. Further, it is important to consider the trophic implications of emulator-based predicted outputs; some emulator results may result in unstable model dynamics if these dynamics occurred in model simulations, for example a 3000 increase in biomass of small pelagics relative to the no oil spill scenario. It is likely that in these cases, the emulator estimate is right at least qualitatively by assigning higher uncertainty to those fish functional groups (Mattern *et al.* 2013). Although the emulators were evaluated against the original Atlantis-GOM model to ensure that sufficient precision was achieved, the acceptable prediction error depends on the specific model application (Guillaume & Guillaume 2014). In this study, our goal was to provide quantitative predictions of temporal changes in biomasses and catch; therefore, our study required higher emulator precision than if our goal had been to assess qualitative general trends.

5. Conclusions

Uncertainty in availability matrix parameters translated into uncertainty in projected biomass and catch under an oil spill scenario. We found that estimation of changes in provisioning ecosystem services (i.e. fisheries catch) and recovery of the fish functional groups

targeted by commercial fisheries following an oil spill were dependent on the composition of predator diets. As model simulations are used to ascertain ecological damage from oil spills and assess tradeoffs, uncertainty analysis can provide decision-makers with comprehensive information regarding possible outcomes, such that they can take well-justified choices. Our results offer insights into the impact of estimation uncertainty on model output and allow for extending our approach into a sensitivity analysis that determines the impact of specific inputs on model simulations related to the food web.

We used statistical emulators to facilitate uncertainty quantification of the availability matrix parameters in the Atlantis-GOM end-to-end ecosystem model, which is capable of assessing ecosystem-level changes resulting from oil exposure, from adverse impacts on organisms to population-level effects, by integrating across biological scales (Coleman *et al.* 2014). We found that the resulting emulators were robust and straightforward to create, which makes them ideal for uncertainty analysis of ecosystem models; this approach could be expanded for sensitivity analysis (i.e. the role of specific parameters), parameter optimization, and calibration of these large, complex deterministic models (Gong *et al.* 2015), and to expand the characterization of uncertainty for management scenarios and allow comparisons between results based on parameter uncertainty and "bounded parameterizations" that simulate "optimistic" and "pessimistic" outcomes (Fulton *et al.* 2011).

Acknowledgements

We would like to thank A. Wallace for having created the food web diagram. Graphical abstract icons courtesy of M. Weijerman, and T. Saxby, J. Hawkey, and D. Tracey. Integration and Application Network, University of Maryland Center for Environmental Science (ian.umces.edu/imagelibrary/). Participants to the Food web ecology workshop, organized by the Institute of Marine Research, in Sommarøy, Norway provided insightful comments to this project. H. Morzaria would like to thank the Integrative Marine Ecology Team at the Northwest Fisheries Science Center. Data are publicly available through the Gulf of Mexico Research Initiative Information & Data Cooperative (GRIIDC) at https://data.gulfresearchinitiative.org [DOI:10.7266/N71G0JSG].

Conflicts of interest

None

Funding source

This article is a result of research funded by the National Oceanic and Atmospheric Administration RESTORE Act Science Program under award NA15NOS4510232 to the University of South Florida and award NA15NOS4510233 to the University of Miami. Microsoft Azure cloud computing resources were provided by a Microsoft Azure Research Award to Hem Nalini Morzaria-Luna. Development of Atlantis and oil dispersal modeling was made possible by a grant from The Gulf of Mexico Research Initiative to the Center for Integrated Modeling and Analysis of Gulf Ecosystems (C-IMAGE) (GRI2011-I-072). The sponsors had no input into the study design, the collection, analysis and interpretation of data, the writing of the article, nor in the decision to submit the article for publication.

Author contributions

Conceived and designed the experiments: HML, JHT, CHA, AG

Performed the experiments: HML, JHT

Analyzed the data: HML, CHA, JHT, AG

Contributed reagents/materials/analysis tools: HML, CHA, JHT

Wrote the paper: HML, CHA, AG

Designed the software used in analysis: HML, CHA

References

Ainsworth, C.H., I.C. Kaplan, P.S. Levin, R. Cudney-Bueno, E.A. Fulton, M. Mangel, P.J. Turk Boyer, J. Torre, A. Pares-Sierra & H. Morzaria-Luna. 2011. Atlantis model development for the Northern Gulf of California. NOAA Technical Memorandum NMFS-NWFSC-110, Seattle.

Ainsworth, C.H., I.C. Kaplan, P.S. Levin & M. Mangel. 2010. A statistical approach for estimating fish diet compositions from multiple, data sources: Gulf of California case study. Ecol. Appl. 20: 2188–2202.

Ainsworth, C.H., C.B. Paris, N. Perlin, L.N. Dornberger, W.F. Patterson 3rd, E. Chancellor, S. Murawski, D. Hollander, K. Daly, I.C. Romero, F. Coleman & H. Perryman. 2018. Impacts of the Deepwater Horizon oil spill evaluated using an end-to-end ecosystem model. PLoS One 13: e0190840.

Ainsworth, C.H., M.J. Schirripa & H. Morzaria-Luna. 2015. An Atlantis ecosystem model for the Gulf of Mexico supporting Integrated Ecosystem Assessment, NOAA Technical Memorandum NMFS-SEFSC-676. NOAA. NFMS. SFSC, Miami.

Allen, J.I. & E.A. Fulton. 2010. Top-down, bottom-up or middle-out? Avoiding extraneous detail and over-generality in marine ecosystem models. Prog. Oceanogr. 84: 129–133.

Audzijonyte, A., R. Gorton, I. Kaplan & E.A. Fulton. 2017. Atlantis User's Guide. Part I: General Overview, Physics & Ecology. Part II: Socio-Economics, CSIRO living document. CSIRO.

Béal, D., P. Brasseur, J.-M. Brankart, Y. Ourmières & J. Verron. 2010. Characterization of mixing errors in a coupled physical biogeochemical model of the North Atlantic: implications for nonlinear estimation using Gaussian anamorphosis. Ocean Sci. 6: 247–262.

Blower, S.M. & H. Dowlatabadi. 1994. Sensitivity and Uncertainty Analysis of Complex Models of Disease Transmission: An HIV Model, as an Example. Int. Stat. Rev. 62: 229–243.

Brand, E.J., I.C. Kaplan, C.J. Harvey, P.S. Levin, E.A. Fulton, A.J. Hermann & J.C. Field. 2007. A spatially explicit ecosystem model of the California Current's food web and oceanography [WWW Document].

Coleman, F.C., J.P. Chanton & E.P. Chassignet. 2014. Ecological Connectivity in Northeastern Gulf of Mexico--The Deep-C Initiative, p. 1972–1984. *In* International Oil Spill Conference Proceedings. American Petroleum Institute.

Committee on the Effects of the Deepwater Horizon Mississippi Canyon-252 Oil Spill on Ecosystem Services in the Gulf of Mexico, Ocean Studies Board, Division on Earth and Life Studies & National Research Council. 2014. An Ecosystem Services Approach to Assessing the Impacts of the Deepwater Horizon Oil Spill in the Gulf of Mexico. National Academies Press (US), Washington (DC).

Cossarini, G., P.F.J. Lermusiaux & C. Solidoro. 2009. Lagoon of Venice ecosystem: Seasonal dynamics and environmental guidance with uncertainty analyses and error subspace data assimilation. J. Geophys. Res. 114: C06026.

Costanza, R., R. d'Arge, R. de Groot, S. Farber, M. Grasso, B. Hannon, K. Limburg, S. Naeem, R.V. O'Neill, J. Paruelo, R.G. Raskin, P. Sutton & M. van den Belt. 1997. The value of the world's ecosystem services and natural capital. Nature 387: 253.

Costello, M.J., M. Coll, R. Danovaro, P. Halpin, H. Ojaveer & P. Miloslavich. 2010. A census of marine biodiversity knowledge, resources, and future challenges. PLoS One 5: e12110.

De Graaff, T., R.J.C.M. Florax, P. Nijkamp & A. Reggiani. 2001. A General Misspecification Test for Spatial Regression Models: Dependence, Heterogeneity, and Nonlinearity. J. Reg. Sci. 41: 255–276.

De Laender, F., G.H. Olsen, T. Frost, B.E. Grøsvik, M. Grung, B.H. Hansen, A.J. Hendriks, M. Hjorth, C.R. Janssen, C. Klok, T. Nordtug, M. Smit, J. Carroll & L. Camus. 2011. Ecotoxicological mechanisms and models in an impact analysis tool for oil spills. J. Toxicol. Environ. Health A 74: 605–619.

Drexler, M. & C.H. Ainsworth. 2013. Generalized Additive Models Used to Predict Species Abundance in the Gulf of Mexico: An Ecosystem Modeling Tool. PLoS One 8.

Farrington, J.W., K.A. Burns & M.S. Leinen. 2016. Synthesis and crosscutting topics of the GoMRI special issue 204: 213.

Fulton, E.A. 2001. The effects of model structure and complexity on the behaviour and performance of marine ecosystem models. University of Tasmania.

Fulton, E.A., J.S. Link, I.C. Kaplan, M. Savina-Rolland, P. Johnson, C.H. Ainsworth, P. Horne, R. Gorton, R. Gamble, A.D.M. Smith & D.C. Smith. 2011. Lessons in modelling and management of marine ecosystems: The Atlantis experience. Fish Fish 12: 171–188.

Fulton, E.A., J.S. Parslow, A.D.M. Smith & C.R. Johnson. 2004. Biogeochemical marine ecosystem models. 2. The effect of physiological data on model performance. Ecol. Modell. 173: 371–406.

Fulton, E.A., A.D.M. Smith & C.R. Johnson. 2004. Biogeochemical marine ecosystem models I: IGBEM - a model of marine bay ecosystems. Ecol. Modell. 174: 267–307.

Garza-Gil, M.D., A. Prada-Blanco & M.X. Vázquez-Rodríguez. 2006. Estimating the short-term economic damages from the Prestige oil spill in the Galician fisheries and tourism. Ecol. Econ. 58: 842–849.

Gong, W., Q. Duan, J. Li, C. Wang, Z. Di, Y. Dai, A. Ye & C. Miao. 2015. Multi-objective parameter optimization of common land model using adaptive surrogate modeling. Hydrol. Earth Syst. Sci. 19: 2409–2425.

Grüss, A., E.A. Babcock, S.R. Sagarese, M. Drexler, D.D. Chagaris, C.H. Ainsworth, B. Penta, S. deRada & T.T. Sutton. 2016. Improving the spatial allocation of functional group biomasses in spatially-explicit ecosystem models: insights from three Gulf of Mexico models. Bull. Mar. Sci. 92: 473–496.

Guillaume, M. & S. Guillaume. 2014. Extending the use of ecological models without sacrificing details: a generic and parsimonious meta-modelling approach. Methods Ecol. Evol. 5: 934–943.

Han, E., H.J. Park, L. Bergamino, K.-S. Choi, E.J. Choy, O.H. Yu, T.W. Lee, H.-S. Park, W.J. Shim & C.-K. Kang. 2015. Stable isotope analysis of a newly established macrofaunal food web 1.5 years after the Hebei Spirit oil spill. Mar. Pollut. Bull. 90: 167–180.

Hayes, K.R., J.M. Dambacher, G.R. Hosack, N.J. Bax, P.K. Dunstan, E.A. Fulton, P.A. Thompson, J.R. Hartog, A.J. Hobday, R. Bradford, S.D. Foster, P. Hedge, D.C. Smith & C.J. Marshall. 2015. Identifying indicators and essential variables for marine ecosystems. Ecol. Indic. 57: 409–419.

Iman, R.L. & J.C. Helton. 1988. An investigation of uncertainty and sensitivity analysis techniques for computer models. Risk Anal.

Kaplan, I.C., P.J. Horne & P.S. Levin. 2012. Screening California Current fishery management scenarios using the Atlantis end-to-end ecosystem model. Prog. Oceanogr. 102: 5–18.

Kohavi, R. 1995. A study of cross-validation and bootstrap for accuracy estimation and model selection, p. 1137–1145. *In* Ijcai. Stanford, CA.

Köhler, P. & K.W. Wirtz. 2002. Linear understanding of a huge aquatic ecosystem model using a group-collecting sensitivity analysis. Environmental Modelling & Software 17: 613–625.

Larsen, L.-H., K. Sagerup & S. Ramsvatn. 2016. The mussel path -- Using the contaminant tracer, Ecotracer, in Ecopath to model the spread of pollutants in an Arctic marine food web. Ecol. Modell. 331: 77–85.

Lassalle, G., P. Bourdaud, B. Saint-Béat, S. Rochette & N. Niquil. 2014. A toolbox to evaluate data reliability for whole-ecosystem models: Application on the Bay of Biscay continental shelf food-web model. Ecol. Modell. 285: 13–21.

Link, J.S., T.F. Ihde, C.J. Harvey, S.K. Gaichas, J.C. Field, J.K.T. Brodziak, H.M. Townsend & R.M. Peterman. 2012. Dealing with uncertainty in ecosystem models: The paradox of use for living marine resource management. Prog. Oceanogr. 102: 102–114.

Liquete, C., C. Piroddi, E.G. Drakou, L. Gurney, S. Katsanevakis, A. Charef & B. Egoh. 2013. Current status and future prospects for the assessment of marine and coastal ecosystem services: a systematic review. PLoS One 8: e67737.

Marino, S., I.B. Hogue, C.J. Ray & D.E. Kirschner. 2008. A methodology for performing global uncertainty and sensitivity analysis in systems biology. J. Theor. Biol. 254: 178–196.

Martin, P.J. 2000. Description of the Navy Coastal Ocean Model Version 1.0. NRL/FR/ 7322-00-9962. Naval Research Laboratory.

Masi, M.D., C.H. Ainsworth & D. Chagaris. 2014. A probabilistic representation of fish diet compositions from multiple data sources: A Gulf of Mexico case study. Ecol. Modell. 284: 60–74.

Mateus, M.D. & G. Franz. 2015. Sensitivity Analysis in a Complex Marine Ecological Model. Water 7: 2060–2081.

Mattern, J.P., K. Fennel & M. Dowd. 2013. Sensitivity and uncertainty analysis of model hypoxia estimates for the Texas-Louisiana shelf. J. Geophys. Res. C: Oceans 118: 1316–1332.

Mattern, J.P., K. Fennel & M. Dowd. 2014. Periodic time-dependent parameters improving forecasting abilities of biological ocean models. Geophys. Res. Lett. 41: 6848–6854.

Millenium Ecosystem Assessment. 2006. Millennium Ecosystem Assessment: Ecosystems And Human-well Being--biodiversity Synthesis. World Resources Inst.

Morris, D.J., D.C. Speirs, A.I. Cameron & M.R. Heath. 2014. Global sensitivity analysis of an end-to-end marine ecosystem model of the North Sea: Factors affecting the biomass of fish and benthos. Ecol. Modell. 273: 251–263.

Murawski, S.A., J.W. Fleeger, W.F. Patterson III, C. Hu, K. Daly, I. Romero & G.A. Toro-Farmer. 2016. How Did the Deepwater Horizon Oil Spill Affect Coastal and Continental Shelf Ecosystems of the Gulf of Mexico? Oceanography 29: 160–173.

Murawski, S.A., W.T. Hogarth, E.B. Peebles & L. Barbeiri. 2014. Prevalence of External Skin Lesions and Polycyclic Aromatic Hydrocarbon Concentrations in Gulf of Mexico Fishes, Post-Deepwater Horizon. Trans. Am. Fish. Soc. 143: 1084–1097.

Nahrgang, J., P. Dubourg, M. Frantzen, D. Storch, F. Dahlke & J.P. Meador. 2016. Early life stages of an arctic keystone species (Boreogadus saida) show high sensitivity to a water-soluble fraction of crude oil. Environ. Pollut. 218: 605–614.

Niiranen, S., T. Blenckner, O. Hjerne & M.T. Tomczak. 2012. Uncertainties in a Baltic Sea Food-Web Model Reveal Challenges for Future Projections. Ambio 41: 613–625.

Nyamweya, C., E. Sturludottir, T. Tomasson, E.A. Fulton, A. Taabu-Munyaho, M. Njiru & G. Stefansson. 2016. Exploring Lake Victoria ecosystem functioning using the Atlantis modeling framework. Environmental Modelling & Software 86: 158–167.

O'Farrell, H., A. Grüss, S.R. Sagarese, E.A. Babcock & K.A. Rose. 2017. Ecosystem modeling in the Gulf of Mexico: current status and future needs to address ecosystem-based

fisheries management and restoration activities. Rev. Fish Biol. Fish. 27: 587–614.
Passow, U. & R.D. Hetland. 2016. What Happened to All of the Oil? Oceanography 29: 88–95.
Perhar, G. & G.B. Arhonditsis. 2014. Aquatic ecosystem dynamics following petroleum hydrocarbon perturbations: A review of the current state of knowledge. J. Great Lakes Res. 40: 56–72.
Perryman, H.A. 2017. Parameterization of an Ecosystem Model and Application for Assessing the Utility of Gulf of Mexico Pelagic Longline Spatial Closures. University of Miami.
Peterson, C.H., S.D. Rice, J.W. Short, D. Esler, J.L. Bodkin, B.E. Ballachey & D.B. Irons. 2003. Long-term ecosystem response to the Exxon Valdez oil spill. Science 302: 2082–2086.
Pettingill, H. & P. Weimer. 2002. Worlwide deepwater exploration and production: Past, present, and future. Lead. Edge 21: 371–376.
Plagányi, É.E. 2007. Models for an ecosystem approach to fisheries, FAO Fisheries Technical Paper. No. 477. Food and Agriculture Organization of the United Nations, Rome.
Prowse, T.A.A., C.J.A. Bradshaw, S. Delean, P. Cassey, R.C. Lacy, K. Wells, M.E. Aiello-Lammens, H.R. Akçakaya & B.W. Brook. 2016. An efficient protocol for the global sensitivity analysis of stochastic ecological models. Ecosphere 7.
R Core Team. 2017. R: A language and environment for statistical computing. Ver. 3.4. R Foundation for Statistical Computing, Vienna, Austria.
Reed, J., L. Shannon, L. Velez, E. Akoglu, A. Bundy, M. Coll, C. Fu, E.A. Fulton, A. Gruss, G. Halouani, J.J. Heymans, J.E. Houle, E. John, F. Le Loc'h, B. Salihoglu, P. Verley & Y.-J. Shin. 2017. Ecosystem indicators-accounting for variability in species' trophic levels. ICES J. Mar. Sci. 74: 158–169.
Saltelli, A., M. Ratto, T. Andres, F. Campolongo, J. Cariboni, D. Gatelli, M. Saisana & S. Tarantola. 2008. Global Sensitivity Analysis: The Primer. John Wiley & Sons.
Shields, M.D. & J. Zhang. 2016. The generalization of Latin hypercube sampling. Reliab. Eng. Syst. Saf. 148: 96–108.
Silliman, B.R., J. van de Koppel, M.W. McCoy, J. Diller, G.N. Kasozi, K. Earl, P.N. Adams & A.R. Zimmerman. 2012. Degradation and resilience in Louisiana salt marshes after the BP-Deepwater Horizon oil spill. Proc. Natl. Acad. Sci. U. S. A. 109: 11234–11239.
Simons, J.D., M. Yuan, C. Carollo, M. Vega-Cendejas, T. Shirley, M.L.D. Palomares, P. Roopnarine, L. Gerardo Abarca Arenas, A. Ibañez, J. Holmes, C. Mazza Schoonard, R. Hertog, D. Reed & J. Poelen. 2013. Building a fisheries trophic interaction database for management and modeling research in the Gulf of Mexico Large Marine Ecosystem. Bull. Mar. Sci. 89: 135–160.
Smith, M.D., E.A. Fulton & R.W. Day. 2015. Using an Atlantis model of the southern Benguela to explore the response of ecosystem indicators for fisheries management. Environmental Modelling & Software 69: 23–41.
Soto, L.A., A.V. Botello, S. Licea-Durán, M.L. Lizárraga-Partida & A. Yáñez-Arancibia. 2014. The environmental legacy of the Ixtoc-I oil spill in Campeche Sound, southwestern Gulf of Mexico. Frontiers in Marine Science 1: 57.
Storlie, C.B., L.P. Swiler, J.C. Helton & C.J. Sallaberry. 2009. Implementation and evaluation of nonparametric regression procedures for sensitivity analysis of computationally demanding models. Reliab. Eng. Syst. Saf. 94: 1735–1763.
Tarnecki, J.H., A.A. Wallace, J.D. Simons & C.H. Ainsworth. 2016. Progression of a Gulf of Mexico food web supporting Atlantis ecosystem model development. Fish. Res. 179: 237–250.
Taylor, K.E. 2001. Summarizing multiple aspects of model performance in a single diagram. J. Geophys. Res. 106: 7183–7192.
Urrego-Blanco, J.R., N.M. Urban, E.C. Hunke, A.K. Turner & N. Jeffery. 2016. Uncertainty quantification and global sensitivity analysis of the Los Alamos sea ice model. J. Geophys.

Res. C: Oceans 121: 2709–2732.

Uusitalo, L., A. Lehikoinen, I. Helle & K. Myrberg. 2015. An overview of methods to evaluate uncertainty of deterministic models in decision support. Environmental Modelling & Software 63: 24–31.

Vilardy, S.P., J.A. González, B. Martín-López & C. Montes. 2011. Relationships between hydrological regime and ecosystem services supply in a Caribbean coastal wetland: a social-ecological approach. Hydrol. Sci. J. 56: 1423–1435.

Weijerman, M., E.A. Fulton, I.C. Kaplan, R. Gorton, R. Leemans, W.M. Mooij & R.E. Brainard. 2015. An Integrated Coral Reef Ecosystem Model to Support Resource Management under a Changing Climate. PLoS One 10: e0144165.

PREPRINT TEXT. Morzaria-Luna, H.N., C.H. Ainsworth, J.H. Tarnecki, and A. Grüss. 2018. Diet composition uncertainty determines impacts on fisheries following an oil spill. Ecosystem Services. 33(Part B):187-198, 10.1016/j.ecoser.2018.05.002

Supplementary Information

Diet composition uncertainty determines impacts on fisheries following an oil spill

Hem Nalini Morzaria-Luna[1*]

Cameron H. Ainsworth[2]

Joseph H. Tarnecki[3]

Arnaud Grüss[4]

1. CEDO Intercultural, PO Box 44208, Tucson, AZ 8573, USA. Edif. Agustín Cortés, s/n. Puerto Peñasco, Sonora CP 83550, México.
2. College of Marine Science, University of South Florida, 140 7th Avenue South, St. Petersburg, FL 33701, USA. Email: ainsworth@usf.edu. Phone: (727) 553-3373
3. Florida Fish and Wildlife Conservation Commission, Fish and Wildlife Research Institute, 100 8th Ave SE, St. Petersburg, FL 33701, USA. Email: jtarnecki83@gmail.com. Phone: 941 875-1247
4. Department of Marine Biology and Ecology, Rosenstiel School of Marine and Atmospheric Science, University of Miami. 4600 Rickenbacker Causeway. Miami, FL 33149-1031, USA. E-mail: agruss@rsmas.miami.edu. Phone: (305) 421 4262

* Corresponding author. hemnalini@cedointercultural.org

Visiting researcher at the Northwest Fisheries Science Center, NOAA, 2725 Montlake Blvd. E., Seattle, WA 98112, USA

Text S1. Emulator model characteristics and tuning parameters.

We briefly describe the characteristics of each emulator model used:

- The Generalized Linear Model (GLM) is a flexible generalization of linear regression that makes no assumptions on the form of the relationship between the response and predictors (Bolker *et al.* 2009). GLM has been widely used as a meta-model as it is easy to implement, requires limited data, is fast to fit, and it is straightforward to obtain estimates of uncertainty around input values (Coutts & Yokomizo 2013).
- Multivariate Adaptive Regression Splines (Friedman 1991) is a flexible procedure that can model complex, non-linear relationships; it is very effective for uncovering interactions in complex data structure.Bagging uses bootstrap sampling to build an ensemble and predicts the outcome by aggregation. We used as tuning parameters the number of terms and the product degree.
- The Extreme Learning Machine (ELM) is based on the structure of single layer feed-forward networks (SLFNs); traditional SLFNs require adjusting and tuning all parameters while in EML the input weights and hidden layer biases can be randomly assigned. Thus, EML makes no assumption on the functional form of the underlying process, provides fast learning speed with good generalization capacity (Huang *et al.* 2006).
- Tree-based methods do not require specifying the parametric nature of the relationship between the predictor variables and the output and do not require assumptions of linearity (Austin *et al.* 2013). These methods apply binary recursive partitioning to divide the sample into distinct subsets; initially, all possible dichotomization of every continuous (above vs. below a certain threshold) variables are considered (Yu-Wei 2015). The binary partition that results in the greatest reduction in error is selected and the process is then repeated iteratively until a predefined stopping rule is satisfied.
    - The Classification and Regression Trees (CART) algorithm recursively searches for a binary split that partitions the data while minimizing a splitting criterion; bagging uses bootstrapping to create an aggregated model (Breiman *et al.* 1984). CART also underlies the random forest (RF) algorithm, which is a nonparametric tree-based method that employs bootstrap sampling to build an ensemble of classification trees and predicts the outcome by aggregating them (Chen & Ishwaran 2012). We used the number of trees and of predictive variables to split the nodes to tune the RF (Breiman 2001).
    - Boosted Regression Trees (BRT) models are a multivariate statistical technique that automatically fits complex, non-linear interactions between variables; here, a large number of simple binary regression trees are combined using boosting and averaged in a single model that generally outperforms traditional multivariate fitting methods (Elith et al., 2008; Hastie et al., 2011). BRT model fitting was controlled by three factors (1) the learning rate (nu), used to shrink the contribution of each tree as it is added to the mode; (2) the interaction depth, which determines how many independent variables can interact to determine each split; and (3) the number of trees required for optimal prediction.

Text S2. Methods for estimating the contribution of each parameter to the emulator.

Further information can be found in the manual for the R package *caret* and in https://topepo.github.io/caret/variable-importance.html. Variable importance is estimated differently according to the model used:

- Generalized Linear Models: uses the absolute value of the *t*-statistic
- Random Forest: The mean squared error (MSE) is computed on the out-of-bag data for each tree, and then computed again after permuting a variable. The differences are averaged and normalized by the squared error (SE), unless the SE equals 0.
- Bagged Trees: Uses the same methodology as a single tree, applied to all bootstrapped trees and returns the total importance
- Boosted Trees: Uses the same approach as a single tree, but sums the importances over each boosting iteration.
- Multivariate Adaptive Regression Splines (MARS): MARS models include a backwards elimination feature selection routine that looks at reductions in the generalized cross-validation (GCV) estimate of error. The "varImp" function from the R package *caret* tracks the changes in GCV, for each predictor and accumulates the reduction in the statistic when each predictor feature is added to the model. This total reduction is used as the variable importance measure.
- Other models: When there is no model-specific way to estimate importance, the importance of each predictor is evaluated individually using a "filter" approach. For regression, a linear relationship between each predictor and the outcome is evaluated. The R^2 statistic for this model is evaluated against the intercept only null model. This number is returned as a relative measure of variable importance.

Figure S1. Hierarchical cluster analysis depicting diet similarity between Atlantis-GOM functional groups, performed using Bray-Curtis dissimilarity measures. Colored lines indicate statistically similar predators, while black brackets illustrate similar clusters of predators.

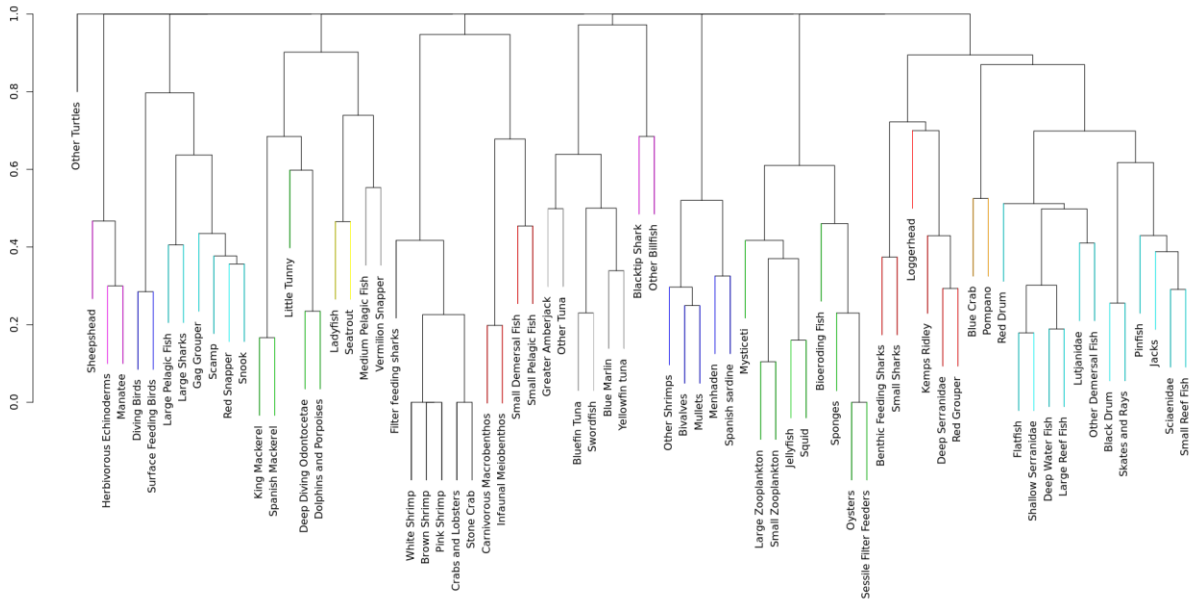

Figure S2. Diet comparison between the fish diet data produced in Tarnecki et al. (2016) and the diet data produced in the present study. Predator functional groups are listed vertically and prey functional groups are listed horizontally. Gray boxes refer to predator-prey linkages that were present in Tarnecki et al. (2016), while black boxes indicate new predator-prey linkages. Predators are presented in order of the number of new prey additions. Comparison of presences/absences of prey and percent diet contributions allow analysis of differences in food web connectivity.

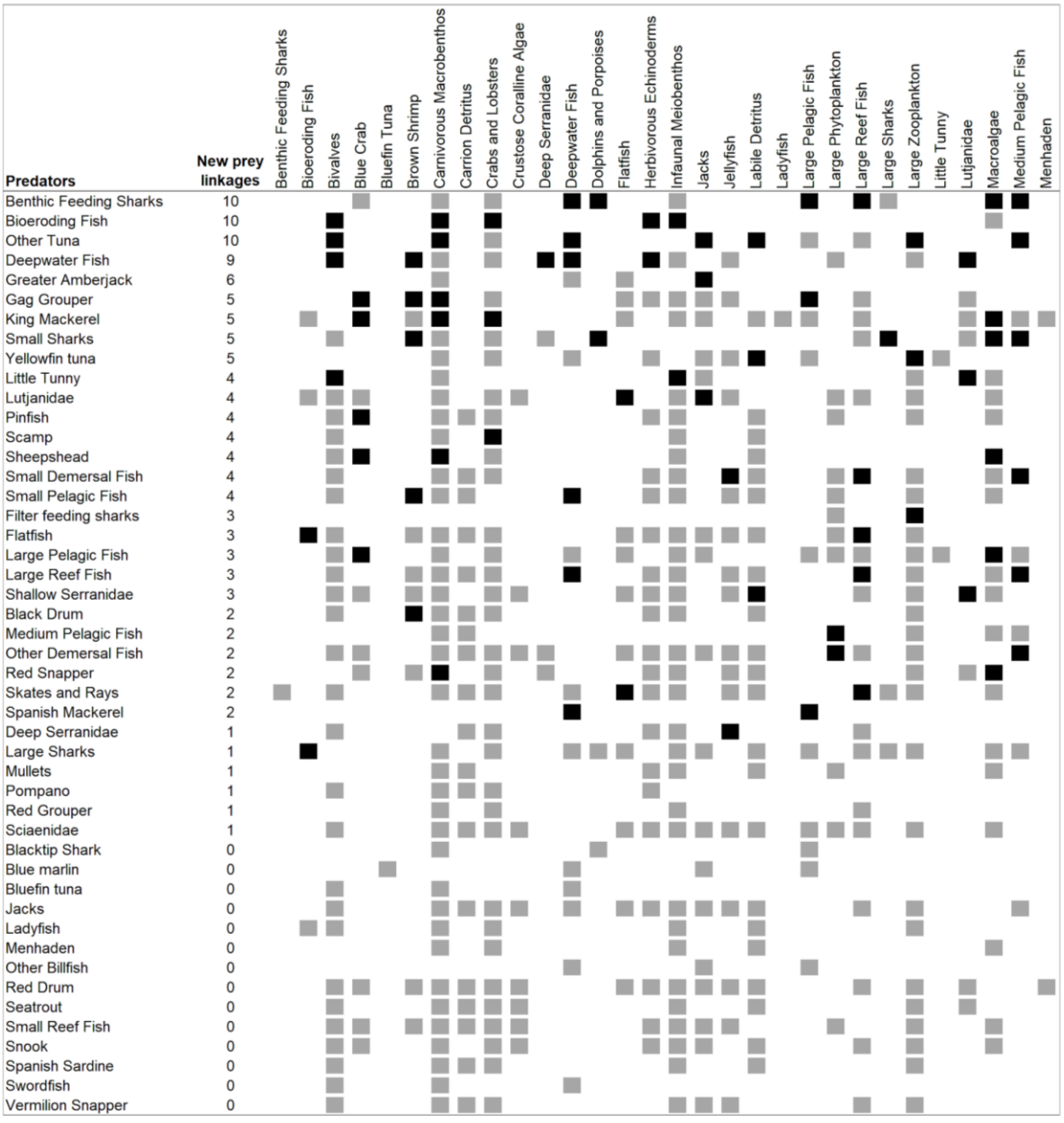

Figure S2 (continued)

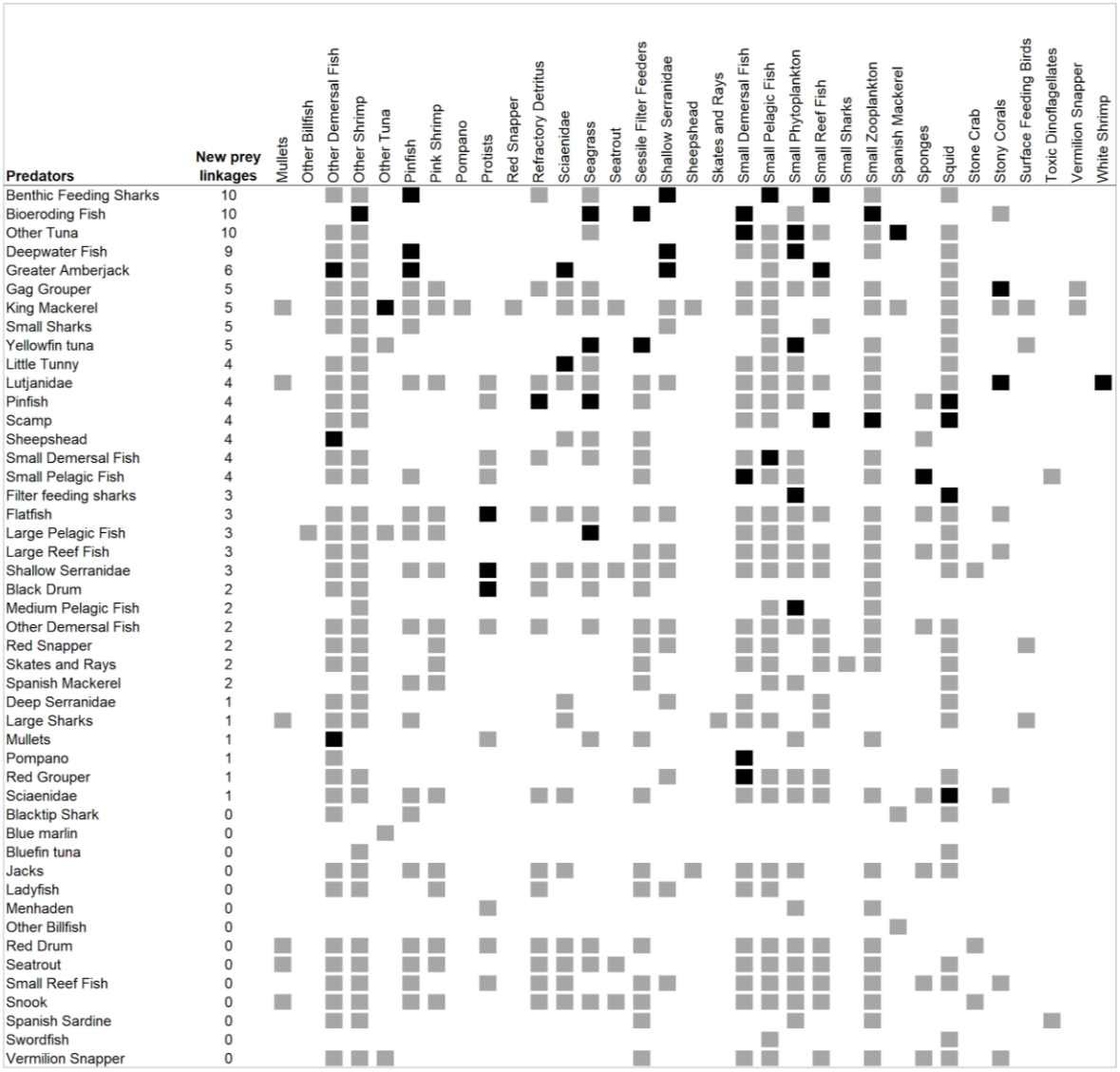

Figure S3. Percent diet composition of the fish functional groups represented in the Atlantis-GOM ecosystem model. Prey items are presented in 12 supergroups.

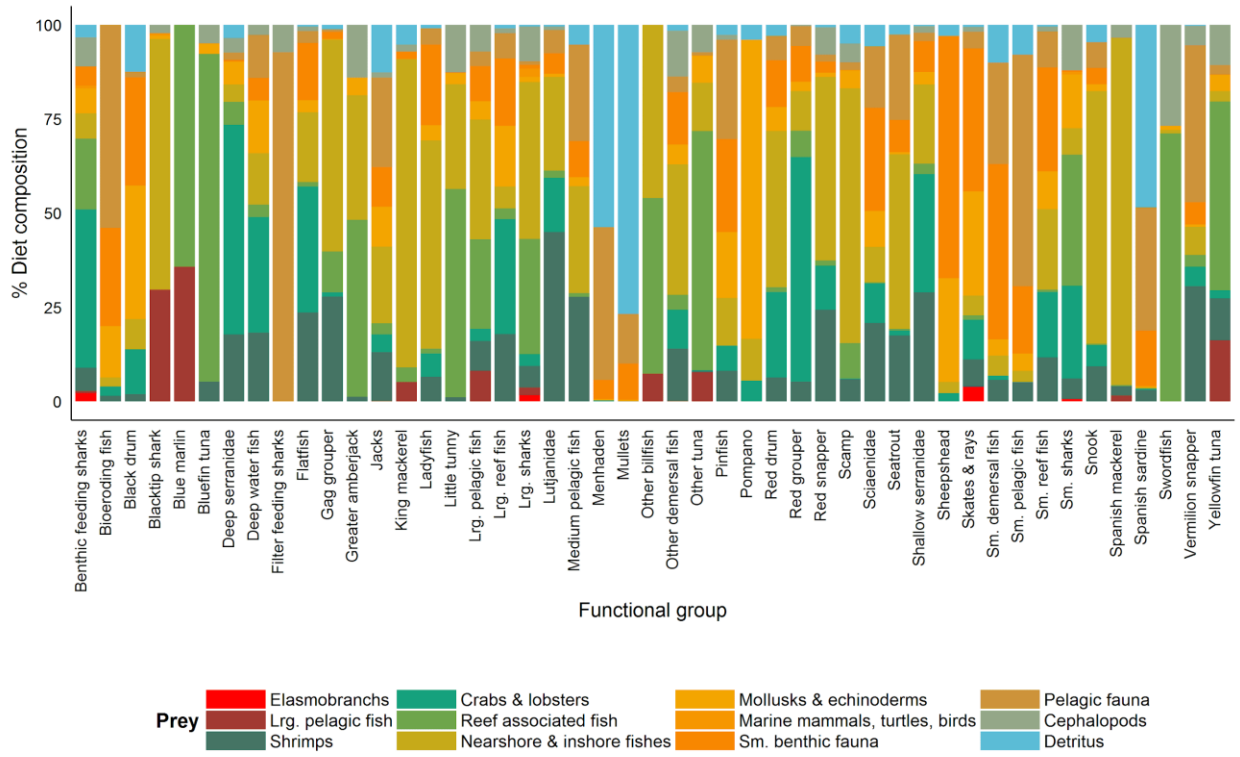

Figure S4. Percent diet composition of Atlantis-GOM fish functional groups. The panels compare diet compositions in the current study with diet compositions in Tarnecki et al. (2016). Prey items are presented in 12 supergroups.

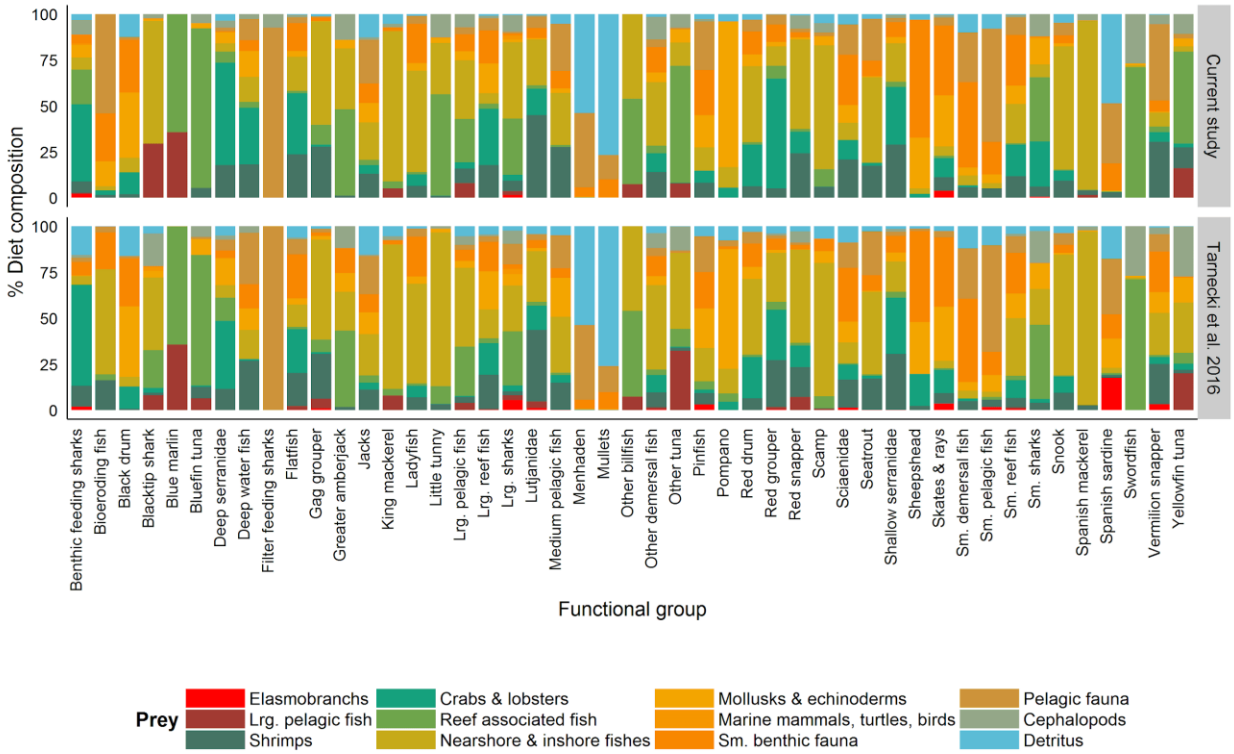

Figure S5. Simulated (A.) and emulated (B.) biomass trajectories for functional groups. The shaded areas in (A.) show the ranges of outcomes observed in the uncertainty analysis of the availability parameters based on 1000 simulations of the Atlantis-GOM ecosystem model which employed a sample of the availability matrices. In (B.), the shaded areas show the ranges of outcomes observed in the uncertainty analysis based on 10,000 emulations of the Atlantis-GOM ecosystem model that reflect the parameter space of availability matrices produced in this study. Note that for the same functional group, the scale of the Y-axis varies. The black lines represent trajectories for the base Atlantis-GOM model, which employs the availability matrix produced in Tarnecki et al. (2016). Species codes are provided in Supplementary Table S4.

A.

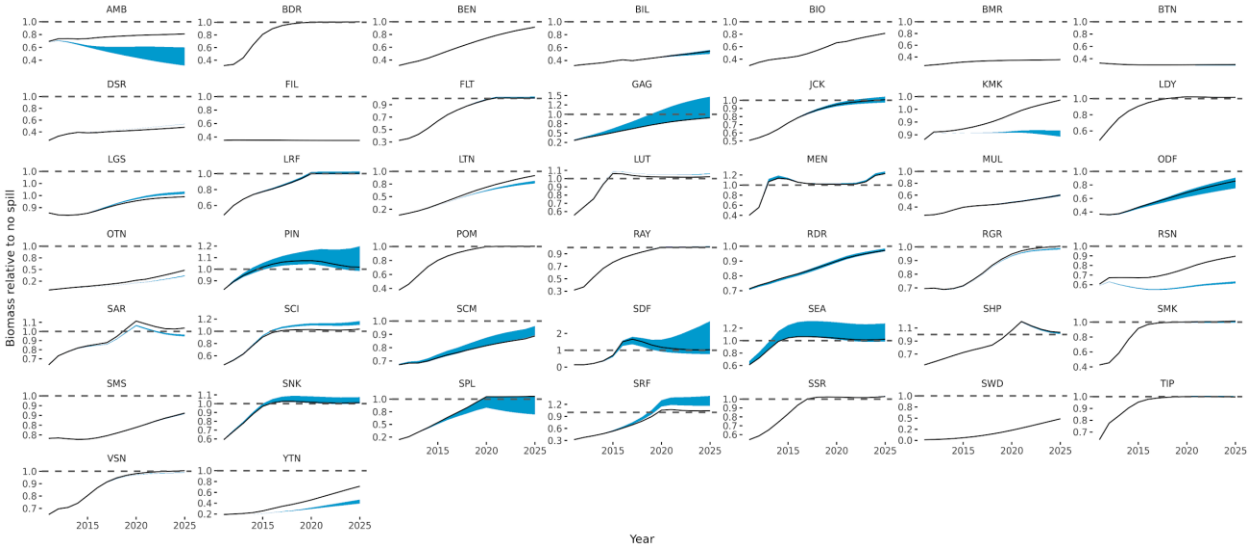

B.

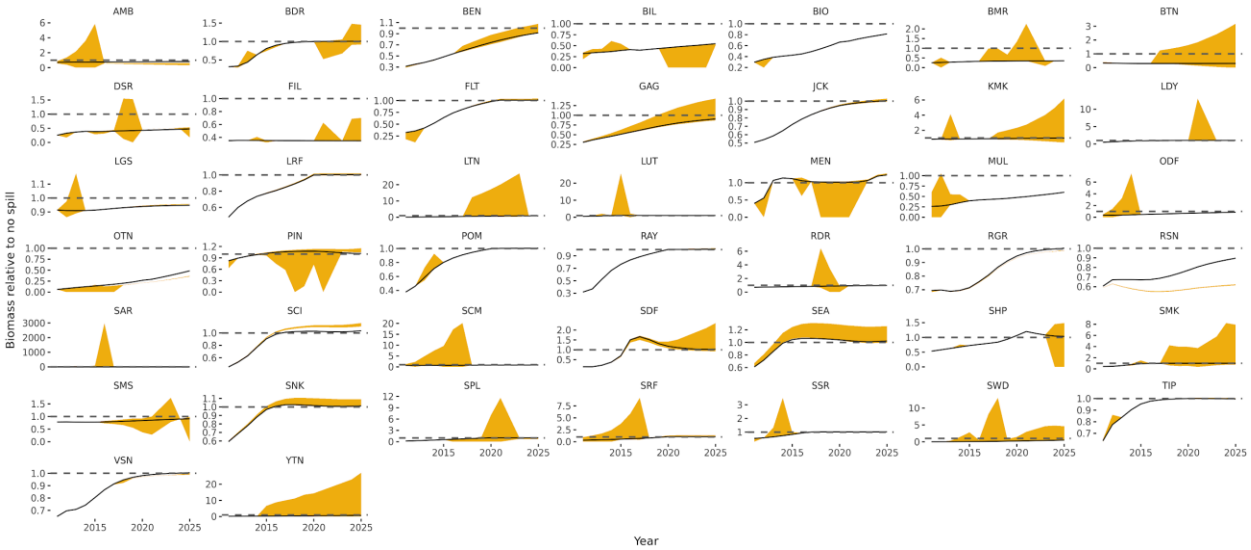

Figure S6. Simulated (A.) and emulated (B.) catch trajectories for Atlantis-GOM functional groups. The shaded areas in (A.) show the ranges of outcomes observed in the uncertainty analysis of the availability parameters based on 1000 simulations of the Atlantis-GOM ecosystem model which employed a sample of the availability matrices. In (B.), the shaded areas show the ranges of outcomes observed in the uncertainty analysis based on 10,000 emulations of the Atlantis-GOM ecosystem model that reflect the parameter space of availability matrices produced in this study. Note that for the same functional group, the scale of the Y-axis varies. The black lines represent trajectories for the base Atlantis-GOM model, which employs the availability matrix produced in Tarnecki et al. (2016). Species codes are provided in Supplementary Table S4.

A.

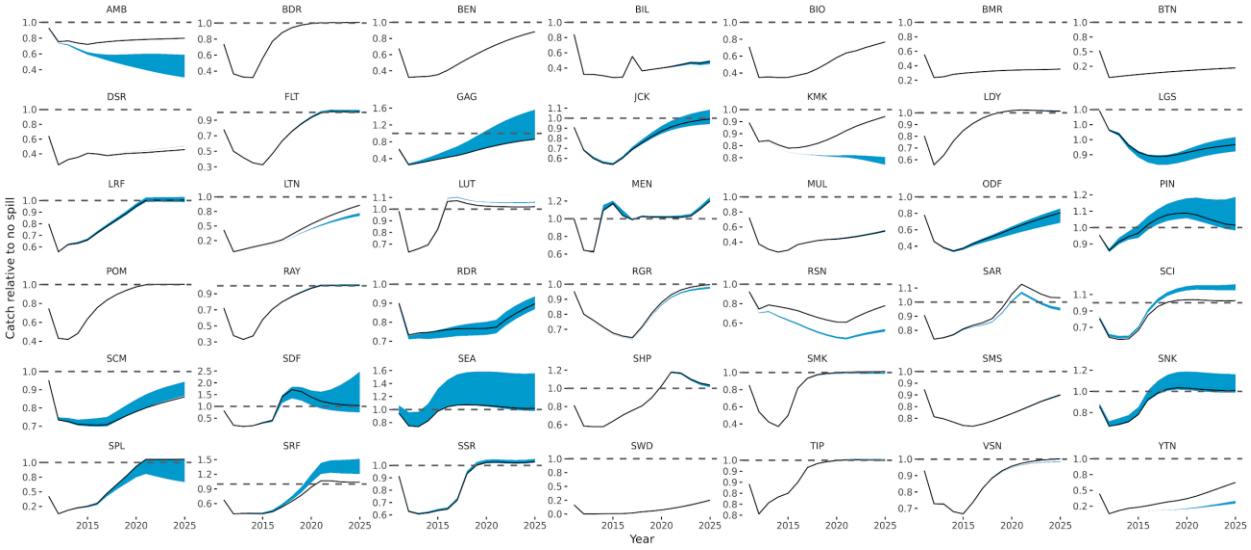

B.

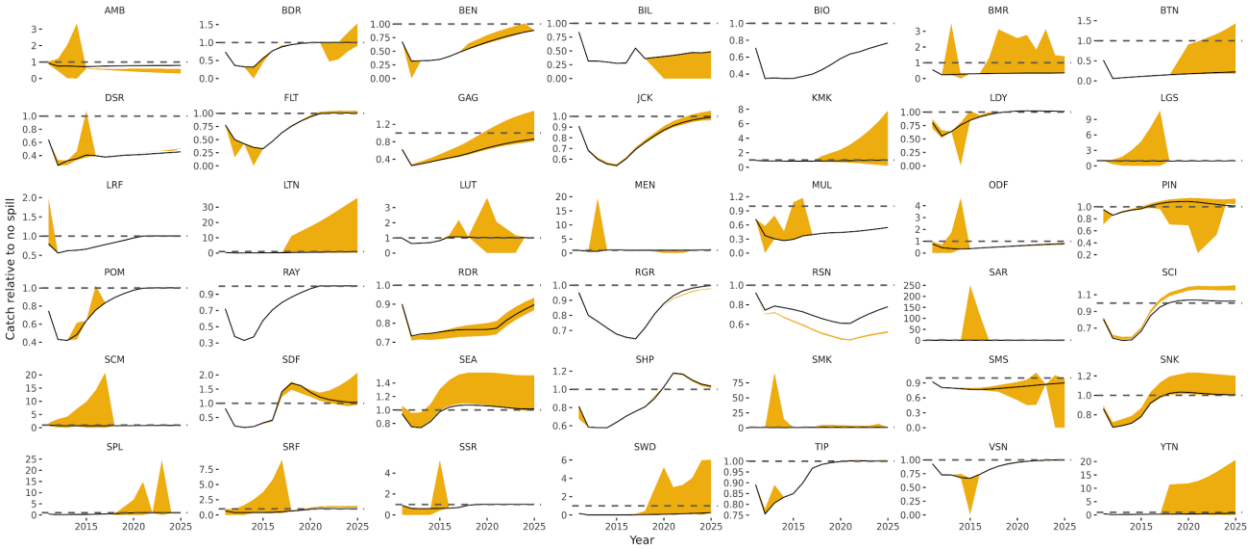

Figure S7. Taylor diagram for biomass (A.) and catch (B.) data by functional group, simulated data for all models tested. The distance from the origin is the normalized standard deviation of Atlantis-GOM modeled biomass. The azimuth angle represents the correlations between the observed Atlantis-GOM simulations, and the distance between the each model symbol and the observations (1 at the X-axis) is the centred root mean square (RMS). Models are: Generalized Linear Model (GLM), Bagged Multivariate Adaptive Regression Splines (BMARS), Bagged Classification and Regression Trees (BCART), Random Forest (RF), Boosted Regression Trees (BRT), and Extreme Learning Machine (ELM). Species codes are provided in Table S4.

A.

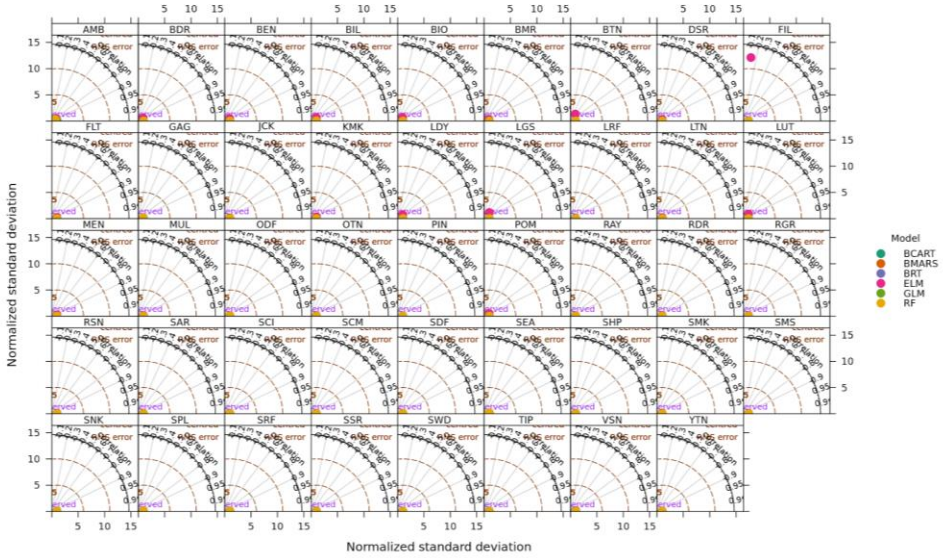

B.

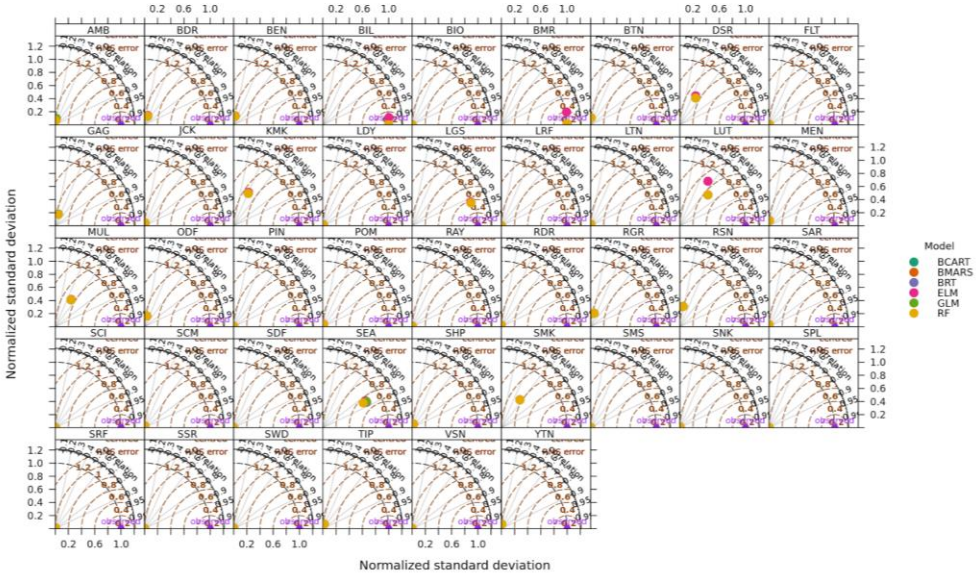

Figure S8. Number of fish stomach samples used on the estimation of diet composition relative to the maximum biomass (A.) and catch (B.) values relative to no oil spill.

A.

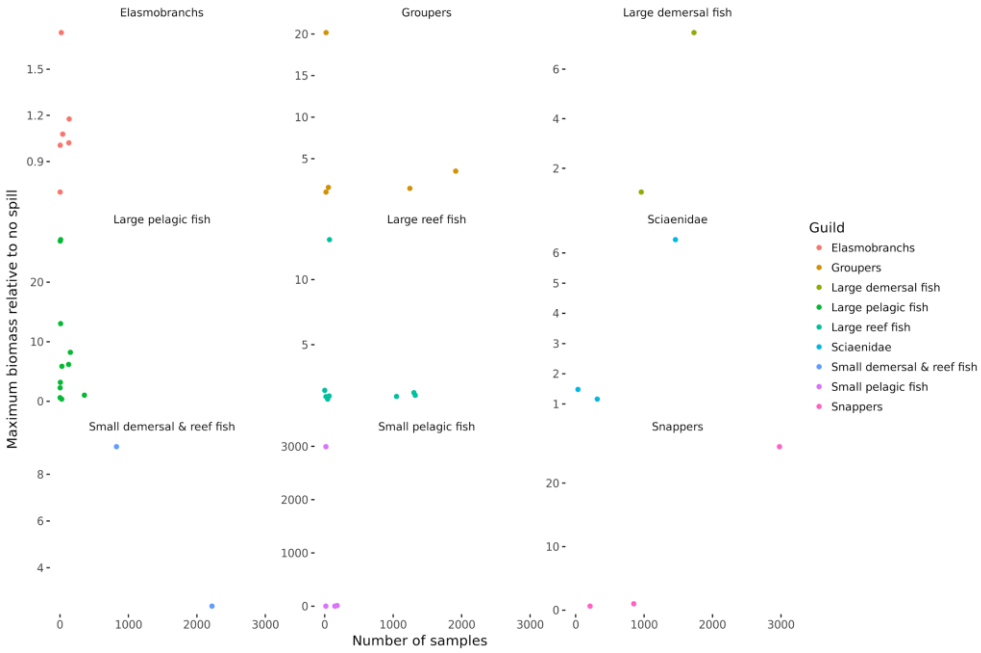

B.

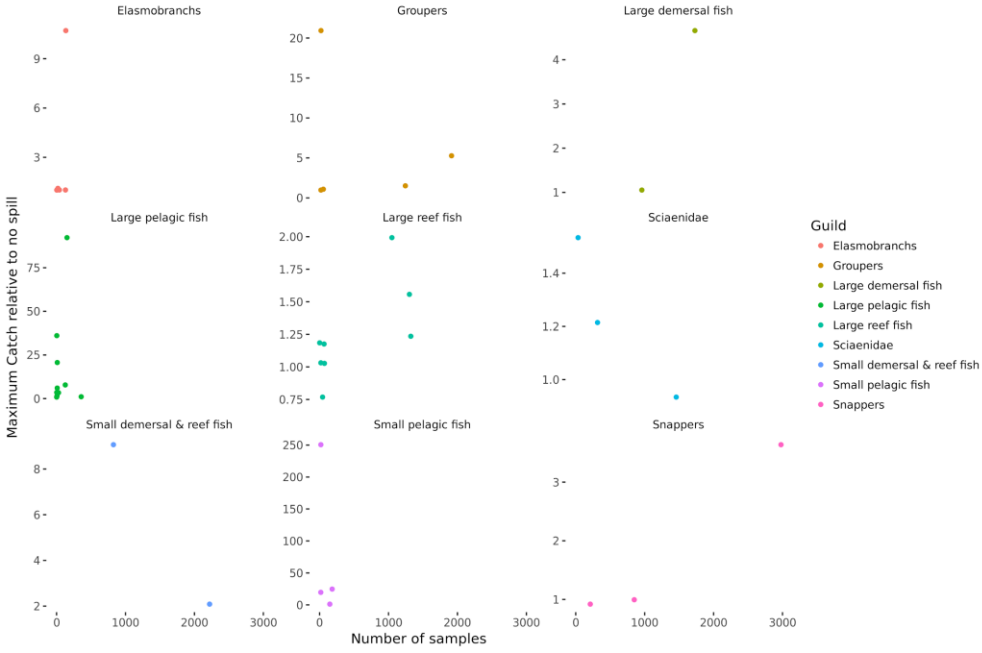

Figure S9. Simulated change in total catch by fisheries fleet for 2011 under the oil spill scenario considered in this study relative to no spill. Bars show mean values and error bars quantify range.

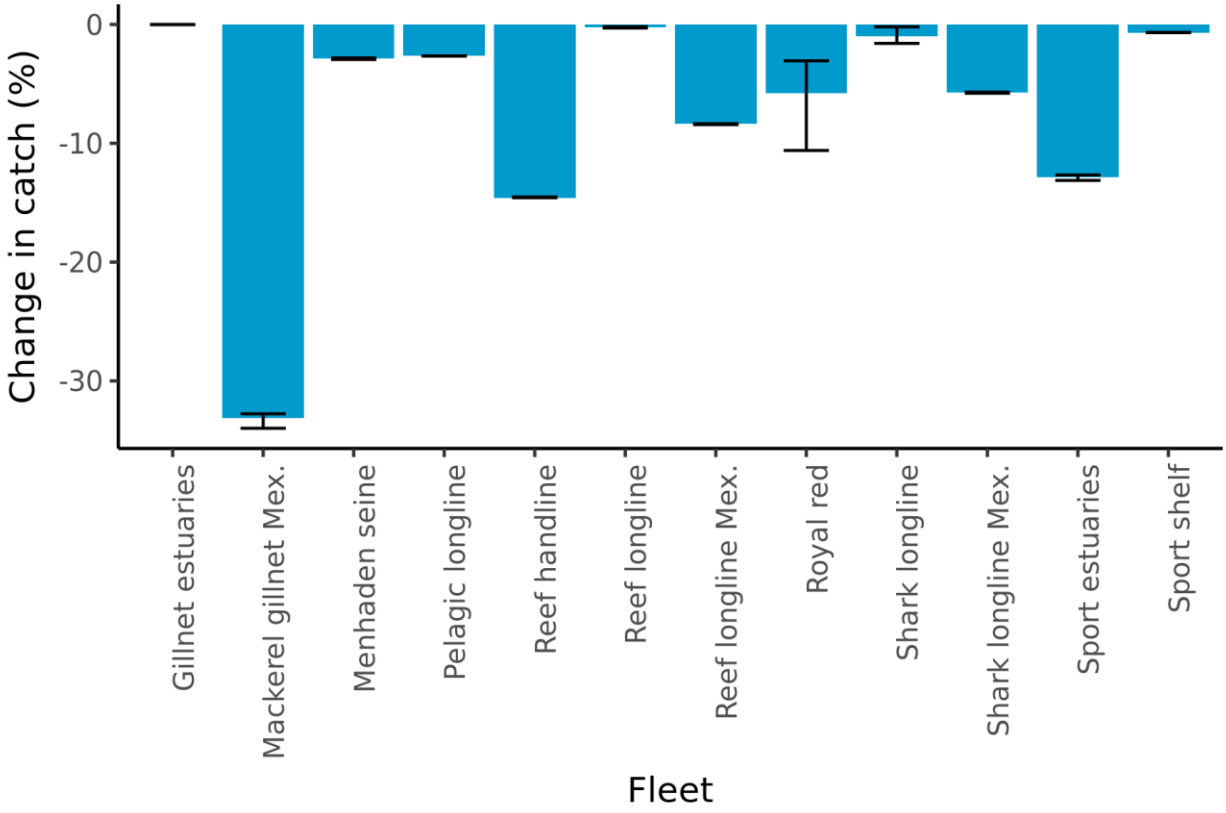

Table S1. R packages used in the data analysis/

Package and use	**Citation**
Tidyverse. Data management and producing figures	Wickham, H., 2016. tidyverse: Easily Install and Load "Tidyverse" Packages. R package version 1.
*Data.tabl*e. Data management	Dowle, M., Srinivasan, A., 2017. data.table: Extension of data.frame.
doSNOW. Parallel computing	Analytics, R., Weston, S., 2014. doSNOW: Foreach parallel adaptor for the snow package. R Package version 1, 12.
Hydromad. Latin hypercube samples were drawn using the function "parameterSets"	Andrews, F., Guillaume, J., 2015. hydromad': hydrological model assessment and development. R package version 0. 9-22. [http://hydromad. catchment. org.
Caret. Generate the emulators	Kuhn, M., Wing, J., Weston, S., Williams, A., Keefer, C., Engelhardt, A., Cooper, T., Mayer, Z., Kenkel, B., Team, R.C., Others, 2014. caret: Classification and regression training. R package version 6.0--21. CRAN: Wien, Austria.
VGAM. Implement the maximum likelihood fitting procedure.	Yee, T.W., Others, 2010. The VGAM package for categorical data analysis. J. Stat. Softw. 32, 1–34.

Table S2. Sources of diet data. (*) Indicates new sources of data relative to (Tarnecki *et al.* 2016)

Source	Samples
Florida Fish and Wildlife Conservation Commission (FWC)'s Fisheries Independent Monitoring (FIM) group based in St. Petersburg, Florida	18,687*
Southeast Area Monitoring and Assessment Program (SEAMAP) program	942*
Gulf of Mexico Species Interactions (GoMexSI) database developed by Texas A&M University in Corpus Christi, Texas (http://gomexsi.tamucc. edu/; (Simons *et al.* 2013)	631
FishBase (Froese & Pauly 2014)	-
(Masi *et al.* 2014))	30*

Table S3. Mode diet distribution, 95% confidence intervals, and numbers of prey (n) for the fish predator functional groups represented in the Atlantis-GOM ecosystem model. This table only includes prey groups that make up at least 1% of the diet of the predators

Benthic Feeding Sharks (n=40)			**Deepwater Fish (Cont.)**			**Large Pelagic Fish (Cont.)**		
Crabs & lobsters	0.42	(0.25, 0.41)	Bivalves	0.04	(0.01, 0.08)	Squid	0.08	(0.02, 0.11)
Small reef fish	0.11	(0.05, 0.14)	Squid	0.02	(0.00, 0.05)	Large pelagic fish	0.07	(0.02, 0.11)
Blue crab	0.09	(0.03, 0.12)	Large zooplankton	0.01	(0.00, 0.05)	Carnivorous macrobenthos	0.05	(0.01, 0.08)
Squid	0.09	(0.03, 0.12)	Small demersal fish	0.01	(0.00, 0.04)	Macroalgae	0.05	(0.01, 0.08)
Carnivorous macrobenthos	0.07	(0.02, 0.10)	Small pelagic fish	0.01	(0.00, 0.04)	Other shrimp	0.04	(0.01, 0.07)
Other shrimp	0.06	(0.02, 0.10)	**Filter feeding sharks (n=2)**			Pink shrimp	0.04	(0.01, 0.07)
Large reef fish	0.04	(0.01, 0.07)	Large zooplankton	0.69	(0.67, 0.70)	Crabs & lobsters	0.03	(0.00, 0.06)
Pinfish	0.03	(0.01, 0.06)	Large phytoplankton	0.16	(0.14, 0.16)	Infaunal meiobenthos	0.02	(0.00, 0.05)
Refractory detritus	0.03	(0.01, 0.06)	Small phytoplankton	0.08	(0.07, 0.08)	Large reef fish	0.02	(0.00, 0.05)
Small pelagic fish	0.02	(0.00, 0.05)	Squid	0.07	(0.06, 0.07)	Small phytoplankton	0.01	(0.00, 0.04)
Infaunal meiobenthos	0.01	(0.00, 0.04)	**Flatfish (n=959)**			**Large Reef Fish (n=1049)**		
Macroalgae	0.01	(0.00, 0.03)	Crabs & lobsters	0.41	(0.24, 0.41)	Crabs & lobsters	0.39	(0.21, 0.39)
Sea grass	0.01	(0.00, 0.03)	Other shrimp	0.28	(0.15, 0.31)	Other shrimp	0.22	(0.11, 0.25)
Shallow serranidae	0.01	(0.00, 0.03)	Infaunal meiobenthos	0.17	(0.08, 0.20)	Infaunal meiobenthos	0.16	(0.07, 0.19)
Bioeroding Fish (43)			Other demersal fish	0.05	(0.01, 0.09)	Carnivorous macrobenthos	0.08	(0.02, 0.12)
Small phytoplankton	0.57	(0.39, 0.56)	Small demersal fish	0.04	(0.01, 0.08)	Bivalves	0.06	(0.02, 0.10)
Macroalgae	0.16	(0.08, 0.20)	Small pelagic fish	0.04	(0.01, 0.08)	Small zooplankton	0.05	(0.01, 0.09)
Carnivorous macrobenthos	0.13	(0.06, 0.17)	Large zooplankton	0.01	(0.00, 0.04)	Herbivorous echinoderms	0.02	(0.00, 0.06)
Infaunal meiobenthos	0.08	(0.03, 0.11)	**Gag Grouper (n=1244)**			Other demersal fish	0.01	(0.00, 0.05)
Small zooplankton	0.05	(0.01, 0.08)	Other demersal fish	0.35	(0.21, 0.37)	Sessile filter feeders	0.01	(0.00, 0.04)
Crabs & lobsters	0.01	(0.00, 0.03)	Other shrimp	0.19	(0.10, 0.23)	**Large Sharks (n=134)**		
Sessile filter feeders	0.01	(0.00, 0.03)	Pinfish	0.13	(0.06, 0.17)	Other demersal fish	0.22	(0.09, 0.24)
Black Drum (n=34)			Pink shrimp	0.11	(0.05, 0.15)	Deep water fish	0.13	(0.05, 0.16)
Infaunal meiobenthos	0.28	(0.19, 0.31)	Small reef fish	0.09	(0.04, 0.13)	Squid	0.12	(0.04, 0.15)
Bivalves	0.27	(0.18, 0.29)	Small pelagic fish	0.07	(0.02, 0.11)	Large reef fish	0.10	(0.03, 0.14)
Crabs & lobsters	0.12	(0.07, 0.15)	Small demersal fish	0.05	(0.01, 0.09)	Small reef fish	0.09	(0.03, 0.13)
Carnivorous macrobenthos	0.09	(0.04, 0.11)	**Greater Amberjack (n=28)**			Pinfish	0.09	(0.02, 0.13)
Other demersal fish	0.08	(0.04, 0.11)	Deep water fish	0.42	(0.23, 0.42)	Small demersal fish	0.08	(0.02, 0.12)
Labile detritus	0.06	(0.02, 0.08)	Small pelagic fish	0.19	(0.08, 0.23)	Other shrimp	0.06	(0.01, 0.10)
Carrion detritus	0.05	(0.02, 0.08)	Squid	0.17	(0.07, 0.21)	Small pelagic fish	0.06	(0.01, 0.10)
Other shrimp	0.02	(0.00, 0.04)	Flatfish	0.08	(0.02, 0.13)	Crabs & lobsters	0.02	(0.00, 0.06)
Sessile filter feeders	0.02	(0.00, 0.04)	Jacks	0.06	(0.02, 0.11)	Carnivorous macrobenthos	0.01	(0.00, 0.04)
Blacktip Shark (n=3)			Carnivorous macrobenthos	0.05	(0.01, 0.09)	Large pelagic fish	0.01	(0.00, 0.04)
Other demersal fish	0.33	(0.30, 0.35)	Other demersal fish	0.01	(0.00, 0.05)	Jacks	0.01	(0.00, 0.04)
Large pelagic fish	0.29	(0.26, 0.31)	Pinfish	0.01	(0.00, 0.05)	**Little Tunny (n=3)**		
Spanish mackerel	0.24	(0.21, 0.26)	Shallow serranidae	0.01	(0.00, 0.04)	Jacks	0.55	(0.52, 0.56)
Pinfish	0.09	(0.07, 0.10)	Small reef fish	0.01	(0.00, 0.04)	Small pelagic fish	0.27	(0.25, 0.28)
Squid	0.02	(0.01, 0.03)	**Jacks (n=357)**			Squid	0.13	(0.11, 0.13)
Carnivorous macrobenthos	0.01	(0.00, 0.01)	Small zooplankton	0.25	(0.11, 0.27)	Carnivorous macrobenthos	0.03	(0.02, 0.03)
Dolphins and porpoises	0.01	(0.00, 0.01)	Small pelagic fish	0.18	(0.07, 0.22)	Other shrimp	0.01	(0.00, 0.01)
Blue marlin (n=2)			Other shrimp	0.14	(0.05, 0.18)	**Lutjanidae (n=2978)**		
Large pelagic fish	0.34	(0.47, 0.51)	Infaunal meiobenthos	0.13	(0.04, 0.17)	Crabs & lobsters	0.16	(0.31, 0.49)
Jacks	0.14	(0.31, 0.35)	Labile detritus	0.13	(0.04, 0.17)	Other demersal fish	0.12	(0.07, 0.20)
Deep water fish	0.05	(0.12, 0.15)	Carnivorous macrobenthos	0.06	(0.01, 0.10)	Small demersal fish	0.12	(0.05, 0.16)
Bluefin tuna	0.01	(0.00, 0.01)	Bivalves	0.04	(0.01, 0.09)	Infaunal meiobenthos	0.05	(0.05, 0.16)
Other tuna	0.01	(0.00, 0.00)	Crabs & lobsters	0.04	(0.00, 0.08)	Other shrimp	0.05	(0.01, 0.09)
Bluefin tuna (n=5)			Large zooplankton	0.04	(0.00, 0.08)	Pink shrimp	0.03	(0.00, 0.07)
Deep water fish	0.87	(0.86, 0.87)	**King Mackerel (n=126)**			Small zooplankton	0.02	(0.00, 0.05)
Other shrimp	0.05	(0.04, 0.05)	Small pelagic fish	0.93	(0.72, 0.86)	Large zooplankton	0.01	(0.00, 0.04)
Squid	0.02	(0.04, 0.05)	Labile detritus	0.04	(0.01, 0.08)	**Medium Pelagic Fish (n=19)**		
Carnivorous macrobenthos	0.02	(0.02, 0.02)	Large pelagic fish	0.02	(0.00, 0.05)	Other shrimp	0.30	(0.22, 0.33)
Deep Serranidae (n=54)			Squid	0.01	(0.00, 0.03)	Small pelagic fish	0.30	(0.22, 0.33)
Crabs & lobsters	0.68	(0.46, 0.64)	**Ladyfish (n=70)**			Small zooplankton	0.24	(0.16, 0.27)
Other shrimp	0.21	(0.11, 0.24)	Small pelagic fish	0.41	(0.29, 0.43)	Macroalgae	0.09	(0.05, 0.12)
Small reef fish	0.05	(0.01, 0.09)	Infaunal meiobenthos	0.22	(0.13, 0.25)	Carrion detritus	0.03	(0.01, 0.05)
Herbivorous echinoderms	0.04	(0.01, 0.08)	Small demersal fish	0.20	(0.12, 0.23)	Large zooplankton	0.03	(0.01, 0.05)
Squid	0.02	(0.00, 0.05)	Crabs & lobsters	0.06	(0.02, 0.09)	Carnivorous macrobenthos	0.01	(0.00, 0.03)
Carrion detritus	0.01	(0.00, 0.04)	Other shrimp	0.05	(0.02, 0.08)	**Menhaden (n=17)**		
Other demersal fish	0.01	(0.00, 0.03)	Large zooplankton	0.04	(0.01, 0.07)	Labile detritus	0.55	(0.50, 0.56)
Deepwater Fish (n=108)			Bivalves	0.02	(0.00, 0.04)	Small zooplankton	0.28	(0.24, 0.29)
Crabs & lobsters	0.37	(0.22, 0.38)	Carnivorous macrobenthos	0.01	(0.00, 0.03)	Small phytoplankton	0.11	(0.09, 0.13)
Other shrimp	0.22	(0.11, 0.24)	**Large Pelagic Fish (n=48)**			Infaunal meiobenthos	0.03	(0.02, 0.04)
Carnivorous macrobenthos	0.09	(0.03, 0.12)	Deep water fish	0.18	(0.08, 0.20)	Macroalgae	0.01	(0.00, 0.02)
Small zooplankton	0.09	(0.03, 0.12)	Other demersal fish	0.16	(0.07, 0.19)	Protists	0.01	(0.00, 0.01)
Other demersal fish	0.08	(0.03, 0.12)	Small pelagic fish	0.16	(0.07, 0.19)	**Mullets (n=65)**		
Infaunal meiobenthos	0.06	(0.02, 0.10)	Jacks	0.08	(0.03, 0.12)	Labile detritus	0.83	(0.68, 0.80)

Mullets (Cont.)		
Small zooplankton	0.11	(0.06, 0.14)
Infaunal meiobenthos	0.02	(0.00, 0.04)
Macroalgae	0.02	(0.00, 0.04)
Small phytoplankton	0.02	(0.00, 0.04)
Other Billfish (n=1)		
Spanish mackerel	0.46	(0.39, 0.39)
Jacks	0.40	(0.45, 0.45)
Deep water fish	0.07	(0.07, 0.07)
Large pelagic fish	0.07	(0.06, 0.06)
Other Demersal Fish (n=1729)		
Small demersal fish	0.30	(0.14, 0.31)
Other shrimp	0.17	(0.07, 0.21)
Squid	0.15	(0.06, 0.19)
Infaunal meiobenthos	0.13	(0.05, 0.17)
Crabs & lobsters	0.12	(0.04, 0.16)
Other demersal fish	0.10	(0.03, 0.14)
Carnivorous macrobenthos	0.03	(0.00, 0.07)
Large zooplankton	0.01	(0.00, 0.04)
Other Tuna (n=25)		
Deep water fish	0.30	(0.22, 0.32)
Medium pelagic fish	0.28	(0.20, 0.30)
Spanish mackerel	0.10	(0.06, 0.13)
Squid	0.08	(0.04, 0.10)
Large pelagic fish	0.07	(0.03, 0.09)
Jacks	0.06	(0.03, 0.09)
Bivalves	0.05	(0.02, 0.07)
Carnivorous macrobenthos	0.02	(0.00, 0.04)
Small reef fish	0.02	(0.00, 0.04)
Small pelagic fish	0.01	(0.00, 0.02)
Pinfish (n=148)		
Infaunal meiobenthos	0.18	(0.08, 0.21)
Small zooplankton	0.13	(0.05, 0.17)
Other demersal fish	0.12	(0.04, 0.15)
Small phytoplankton	0.11	(0.04, 0.15)
Other shrimp	0.09	(0.03, 0.13)
Macroalgae	0.08	(0.02, 0.12)
Carnivorous macrobenthos	0.07	(0.02, 0.11)
Crabs & lobsters	0.07	(0.02, 0.11)
Bivalves	0.05	(0.01, 0.09)
Herbivorous echinoderms	0.05	(0.01, 0.08)
Large zooplankton	0.03	(0.00, 0.07)
Pompano (n=18)		
Carnivorous macrobenthos	0.46	(0.31, 0.47)
Bivalves	0.39	(0.25, 0.41)
Small demersal fish	0.04	(0.01, 0.07)
Carrion detritus	0.03	(0.01, 0.07)
Crabs & lobsters	0.03	(0.01, 0.07)
Herbivorous echinoderms	0.03	(0.00, 0.06)
Other demersal fish	0.03	(0.00, 0.06)
Red Drum (n=1458)		
Crabs & lobsters	0.29	(0.13, 0.30)
Other demersal fish	0.24	(0.10, 0.26)
Pinfish	0.18	(0.07, 0.21)
Infaunal meiobenthos	0.09	(0.02, 0.13)
Large zooplankton	0.04	(0.01, 0.08)
Small demersal fish	0.04	(0.00, 0.08)
Herbivorous echinoderms	0.03	(0.00, 0.07)
Other shrimp	0.03	(0.00, 0.07)
Sea grass	0.02	(0.00, 0.06)
Small pelagic fish	0.02	(0.00, 0.06)
Pink shrimp	0.01	(0.00, 0.05)
Red Grouper (n=19)		
Crabs & lobsters	0.66	(0.53, 0.65)
Infaunal meiobenthos	0.09	(0.05, 0.12)
Small reef fish	0.06	(0.03, 0.09)
Other demersal fish	0.05	(0.02, 0.08)
Pink shrimp	0.05	(0.02, 0.07)
Small pelagic fish	0.03	(0.01, 0.06)
Small phytoplankton	0.03	(0.01, 0.05)
Carnivorous macrobenthos	0.02	(0.00, 0.04)
Red Snapper (n=211)		
Other demersal fish	0.49	(0.33, 0.49)
Other shrimp	0.26	(0.16, 0.29)
Crabs & lobsters	0.13	(0.06, 0.16)
Squid	0.07	(0.03, 0.11)
Small demersal fish	0.03	(0.00, 0.06)
Infaunal meiobenthos	0.02	(0.00, 0.04)

Scamp (n=20)		
Other demersal fish	0.57	(0.38, 0.55)
Small pelagic fish	0.16	(0.08, 0.20)
Small reef fish	0.10	(0.04, 0.14)
Other shrimp	0.05	(0.02, 0.09)
Labile detritus	0.03	(0.01, 0.07)
Small demersal fish	0.03	(0.00, 0.06)
Squid	0.03	(0.00, 0.06)
Bivalves	0.02	(0.00, 0.05)
Small zooplankton	0.01	(0.00, 0.03)
Sciaenidae (n=316)		
Infaunal meiobenthos	0.31	(0.19, 0.33)
Other shrimp	0.23	(0.13, 0.26)
Crabs & lobsters	0.11	(0.05, 0.14)
Small zooplankton	0.10	(0.04, 0.13)
Carnivorous macrobenthos	0.07	(0.02, 0.10)
Large zooplankton	0.06	(0.02, 0.10)
Labile detritus	0.04	(0.01, 0.08)
Other demersal fish	0.03	(0.01, 0.06)
Bivalves	0.02	(0.00, 0.05)
Small demersal fish	0.02	(0.00, 0.04)
Small pelagic fish	0.01	(0.00, 0.03)
Seatrout (n=1303)		
Small demersal fish	0.32	(0.18, 0.34)
Large zooplankton	0.18	(0.09, 0.22)
Other shrimp	0.15	(0.07, 0.19)
Small pelagic fish	0.15	(0.07, 0.19)
Infaunal meiobenthos	0.08	(0.03, 0.12)
Small zooplankton	0.07	(0.02, 0.11)
Pink shrimp	0.03	(0.00, 0.07)
Refractory detritus	0.01	(0.00, 0.03)
Shallow Serranidae (n=1914)		
Crabs & lobsters	0.38	(0.22, 0.39)
Other shrimp	0.34	(0.19, 0.36)
Other demersal fish	0.10	(0.04, 0.15)
Small demersal fish	0.10	(0.04, 0.14)
Infaunal meiobenthos	0.08	(0.03, 0.12)
Sheepshead (n=1)		
Blue crab	0.89	(0.00, 0.00)
Skates and Rays (n=129)		
Infaunal meiobenthos	0.41	(0.26, 0.41)
Bivalves	0.21	(0.11, 0.24)
Crabs & lobsters	0.12	(0.05, 0.15)
Carnivorous macrobenthos	0.10	(0.04, 0.13)
Other shrimp	0.08	(0.03, 0.11)
Other demersal fish	0.03	(0.01, 0.07)
Sessile filter feeders	0.03	(0.00, 0.06)
Large zooplankton	0.02	(0.00, 0.05)
Small Demersal Fish (n=2220)		
Infaunal meiobenthos	0.55	(0.37, 0.54)
Small zooplankton	0.24	(0.14, 0.27)
Labile detritus	0.06	(0.02, 0.10)
Other shrimp	0.06	(0.02, 0.09)
Carnivorous macrobenthos	0.03	(0.00, 0.06)
Carrion detritus	0.02	(0.00, 0.06)
Small demersal fish	0.02	(0.00, 0.05)
Large zooplankton	0.01	(0.00, 0.04)
Small phytoplankton	0.01	(0.00, 0.03)
Small Pelagic Fish (n=182)		
Small zooplankton	0.45	(0.33, 0.46)
Large zooplankton	0.18	(0.12, 0.21)
Infaunal meiobenthos	0.13	(0.07, 0.16)
Labile detritus	0.07	(0.04, 0.10)
Other shrimp	0.05	(0.02, 0.07)
Sessile filter feeders	0.05	(0.02, 0.07)
Bivalves	0.02	(0.00, 0.04)
Carnivorous macrobenthos	0.02	(0.00, 0.04)
Small phytoplankton	0.02	(0.00, 0.04)
Small pelagic fish	0.01	(0.00, 0.02)
Small Reef Fish (n=825)		
Infaunal meiobenthos	0.30	(0.15, 0.32)
Crabs & lobsters	0.21	(0.09, 0.24)
Small pelagic fish	0.16	(0.06, 0.19)
Other shrimp	0.14	(0.05, 0.18)
Small zooplankton	0.06	(0.01, 0.10)
Bivalves	0.03	(0.00, 0.07)
Carnivorous macrobenthos	0.03	(0.00, 0.07)
Small demersal fish	0.03	(0.00, 0.07)

Small Reef Fish (Cont.)		
Herbivorous echinoderms	0.02	(0.00, 0.06)
Other demersal fish	0.02	(0.00, 0.05)
Small Sharks (n=19)		
Crabs & lobsters	0.28	(0.18, 0.30)
Large reef fish	0.16	(0.10, 0.19)
Carnivorous macrobenthos	0.15	(0.08, 0.17)
Squid	0.14	(0.08, 0.16)
Small reef fish	0.08	(0.03, 0.10)
Deep serranidae	0.03	(0.01, 0.05)
Other demersal fish	0.03	(0.01, 0.05)
Other shrimp	0.03	(0.00, 0.05)
Small pelagic fish	0.03	(0.00, 0.05)
Brown shrimp	0.02	(0.00, 0.05)
Lutjanidae	0.02	(0.00, 0.04)
Shallow serranidae	0.02	(0.00, 0.03)
Bivalves	0.01	(0.00, 0.03)
Pinfish	0.01	(0.00, 0.03)
Snook (n=1323)		
Other demersal fish	0.54	(0.29, 0.50)
Small demersal fish	0.15	(0.05, 0.19)
Other shrimp	0.08	(0.02, 0.12)
Small pelagic fish	0.07	(0.02, 0.12)
Pinfish	0.05	(0.01, 0.10)
Crabs & lobsters	0.04	(0.01, 0.09)
Refractory detritus	0.03	(0.00, 0.07)
Large zooplankton	0.01	(0.00, 0.05)
Pink shrimp	0.01	(0.00, 0.05)
Sea grass	0.01	(0.00, 0.05)
Spanish Mackerel (n=151)		
Small pelagic fish	0.99	(0.86, 0.94)
Squid	0.01	(0.00, 0.03)
Spanish Sardine (n=18)		
Labile detritus	0.50	(0.43, 0.51)
Large zooplankton	0.17	(0.13, 0.19)
Small zooplankton	0.16	(0.12, 0.18)
Sessile filter feeders	0.09	(0.06, 0.10)
Infaunal meiobenthos	0.05	(0.03, 0.06)
Other shrimp	0.03	(0.01, 0.04)
Swordfish (n=9)		
Deep water fish	0.72	(0.69, 0.72)
Squid	0.27	(0.25, 0.27)
Bivalves	0.01	(0.00, 0.01)
Small pelagic fish	0.01	(0.00, 0.00)
Vermilion Snapper (n=849)		
Other shrimp	0.36	(0.23, 0.38)
Large zooplankton	0.26	(0.15, 0.29)
Jellyfish	0.12	(0.05, 0.15)
Small zooplankton	0.09	(0.04, 0.12)
Crabs & lobsters	0.05	(0.01, 0.08)
Infaunal meiobenthos	0.05	(0.01, 0.08)
Small pelagic fish	0.04	(0.01, 0.07)
Squid	0.04	(0.01, 0.07)
Other demersal fish	0.01	(0.00, 0.03)
Yellowfin tuna (n=10)		
Deep water fish	0.51	(0.46, 0.52)
Large pelagic fish	0.16	(0.13, 0.17)
Other shrimp	0.11	(0.09, 0.12)
Squid	0.11	(0.08, 0.12)
Carnivorous macrobenthos	0.04	(0.03, 0.05)
Crabs & lobsters	0.02	(0.01, 0.03)
Small pelagic fish	0.02	(0.01, 0.03)
Small phytoplankton	0.02	(0.01, 0.02)

Table S4. Fish guild composition.

Atlantis-GOM functional group*	Code	Snappers	Groupers	Large pelagic fish	Small pelagic fish	Small demersal & reef fish	Sciaenidae	Elasmobranchs	Large demersal fish	Large reef fish
Gag grouper	GAG		■							
Red grouper	RGR		■							
Scamp	SCM		■							
Shallow serranidae	SSR		■							
Deep serranidae	DSR		■							
Red snapper	RSN	■								
Vermilion snapper	VSN	■								
Lutjanidae	LUT	■								
Bioeroding fish	BIO									■
Large reef fish	LRF									■
Small reef fish	SRF					■				
Black drum	BDR						■			
Red drum	RDR						■			
Seatrout	SEA									■
Sciaenidae	SCI						■			
Ladyfish	LDY									■
Mullets	MUL									■
Pompano	POM									■
Sheepshead	SHP									■
Snook	SNK									■
Flatfish	FLT								■	
Other demersal fish	ODF								■	
Small demersal fish	SDF					■				
Yellowfin tuna	YTN			■						
Bluefin tuna	BTN			■						
Little tunny	LTN			■						
Other tuna	OTN			■						
Swordfish	SWD			■						
White marlin	WMR			■						
Blue marlin	BMR			■						
Other billfish	BIL			■						
Greater amberjack	AMB			■						
Jacks	JCK			■						
King mackerel	KMK			■						
Spanish mackerel	SMK			■						

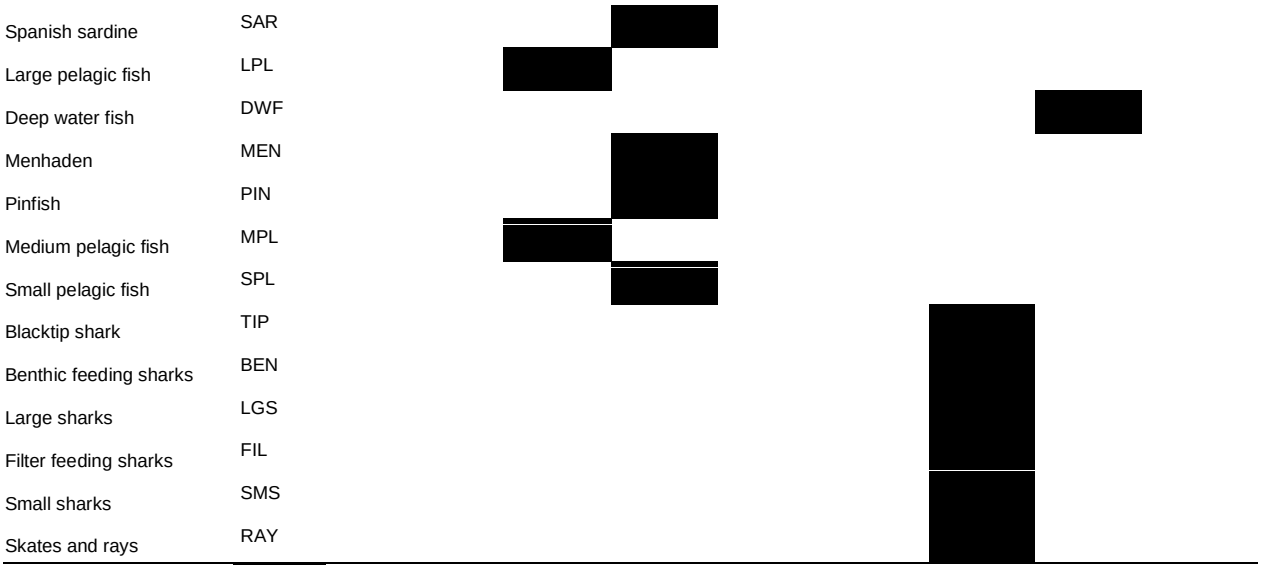

*See (Ainsworth *et al.* 2015) for the lists of species making up each of these functional groups represented in the Atlantis-GOM ecosystem model.

Table S5. Functional groups that did not achieve recovery. Recovery was defined as a return to 99% pre-oil spill biomass within the 15yr time period. Indicates if groups did not achieve recovery in base model (B), simulations (S), and emulations (E).

Run	Guild	Functional group
E, S, B	Elasmobranchs	Filter feeding sharks
E, S, B	Elasmobranchs	Large sharks
B	Groupers	Vermilion snapper
B	Groupers	Gag grouper
B	Groupers	Red snapper
E, S	Large pelagic fish	Other billfish
B	Large pelagic fish	White marlin
E, S,B	Large pelagic fish	Blue marlin
S,B	Large pelagic fish	Bluefin tuna
S,B	Large pelagic fish	King mackerel
S	Large pelagic fish	Spanish mackerel
S,B	Large pelagic fish	Swordfish
E, S	Snappers	Red snapper
E, S	Snappers	Vermilion snapper
E, S, B	Small pelagic fish	Menhaden

References

Ainsworth, C.H., M.J. Schirripa & H. Morzaria-Luna. 2015. An Atlantis ecosystem model for the Gulf of Mexico supporting Integrated Ecosystem Assessment, NOAA Technical Memorandum NMFS-SEFSC-676. NOAA. NFMS. SFSC, Miami.

Austin, P.C., J.V. Tu, J.E. Ho, D. Levy & D.S. Lee. 2013. Using methods from the data-mining and machine-learning literature for disease classification and prediction: a case study examining classification of heart failure subtypes. J. Clin. Epidemiol. 66: 398–407.

Bolker, B.M., M.E. Brooks, C.J. Clark, S.W. Geange, J.R. Poulsen, M.H.H. Stevens & J.-S.S. White. 2009. Generalized linear mixed models: a practical guide for ecology and evolution. Trends Ecol. Evol. 24: 127–135.

Breiman, L. 2001. Random Forests. Machine Learning.

Breiman, L., J. Friedman, C.J. Stone & R.A. Olshen. 1984. Classification and regression trees. CRC press.

Chen, X. & H. Ishwaran. 2012. Random forests for genomic data analysis. Genomics 99: 323–329.

Coutts, S.R. & H. Yokomizo. 2013. Meta-models as a straightforward approach to the sensitivity analysis of complex models. Popul. Ecol. 56: 7–19.

Friedman, J.H. 1991. Multivariate Adaptive Regression Splines. Ann. Stat. 19: 1–67.

Froese, R. & D. Pauly (Eds.). 2014. FishBase. World Wide Web electronic publication. www.fishbase.org, (11/2014).

Huang, G.-B., Q.-Y. Zhu & C.-K. Siew. 2006. Extreme learning machine: Theory and applications. Neurocomputing 70: 489–501.

Masi, M.D., C.H. Ainsworth & D. Chagaris. 2014. A probabilistic representation of fish diet compositions from multiple data sources: A Gulf of Mexico case study. Ecol. Modell. 284: 60–74.

Simons, J.D., M. Yuan, C. Carollo, M. Vega-Cendejas, T. Shirley, M.L.D. Palomares, P. Roopnarine, L. Gerardo Abarca Arenas, A. Ibañez, J. Holmes, C. Mazza Schoonard, R. Hertog, D. Reed & J. Poelen. 2013. Building a fisheries trophic interaction database for management and modeling research in the Gulf of Mexico Large Marine Ecosystem. Bull. Mar. Sci. 89: 135–160.

Tarnecki, J.H., A.A. Wallace, J.D. Simons & C.H. Ainsworth. 2016. Progression of a Gulf of Mexico food web supporting Atlantis ecosystem model development. Fish. Res. 179: 237–250.

Yu-Wei, C. 2015. Machine Learning with R Cookbook. Packt Publishing Ltd.